LANDSCAPES OF FACILITATION: HOW SELF-ORGANIZED PATCHINESS OF AQUATIC MACROPHYTES PROMOTES DIVERSITY IN STREAMS

Loreta Cornacchia[1, 4], Johan van de Koppel[1, 4], Daphne van der Wal[1], Geraldene Wharton[2], Sara Puijalon[3], Tjeerd J. Bouma[1, 4].

[1] NIOZ Royal Netherlands Institute for Sea Research, Department of Estuarine and Delta Systems, and Utrecht University, P.O. Box 140, 4400 AC Yerseke, the Netherlands.

[2] School of Geography, Queen Mary University of London, London, UK

[3] UMR 5023 LEHNA, CNRS, Université Lyon 1, ENTPE, Villeurbanne, France

[4] Groningen Institute for Evolutionary Life Sciences, University of Groningen, PO Box 11103, 9700 CC Groningen, The Netherlands

Abstract

Spatial heterogeneity plays a crucial role in the coexistence of species. Despite recognition of the importance of self-organization in creating environmental heterogeneity in otherwise uniform landscapes, the effects of such self-organized pattern formation in promoting coexistence through facilitation are still unknown. In this study, we investigated the effects of pattern formation on species interactions and community spatial structure in ecosystems with limited underlying environmental heterogeneity, using self-organized patchiness of the aquatic macrophyte *Callitriche platycarpa* in streams as a model system. Our theoretical model predicted that pattern formation in aquatic vegetation – due to feedback interactions between plant growth, water flow and sedimentation processes – could promote species coexistence, by creating heterogeneous flow conditions inside and around the plant patches. The spatial plant patterns predicted by our model agreed with field observations at the reach scale in naturally vegetated rivers, where we found a significant spatial aggregation of two macrophyte species around *C. platycarpa*. Field transplantation experiments showed that *C. platycarpa* had a positive effect on the growth of both beneficiary species, and the intensity of this facilitative effect was correlated with the heterogeneous hydrodynamic conditions created within and around *C. platycarpa* patches. Our results emphasize the importance of self-organized patchiness in promoting species coexistence by creating a landscape of facilitation, where new niches and facilitative effects arise in different locations. Understanding the interplay between competition and facilitation is therefore essential for successful management of biodiversity in many ecosystems.

Keywords: species coexistence; positive interactions; spatial patterns; spatial self-organization; Callitriche platycarpa*; stream macrophytes; patchiness; habitat diversity.*

1 Introduction

The challenge of understanding species diversity and coexistence is fundamental in community ecology. According to the competitive exclusion principle, two species competing for the same resource cannot coexist if other ecological factors are constant (Gause 1932). However, many natural communities defy the theoretical predictions of low species coexistence, as often a high number of species can be found living on few resources (e.g. 'paradox of the plankton', Hutchinson (1961)). To explain this discrepancy, many of the suggested mechanisms rely on the importance of spatial or temporal heterogeneity (Levin 1970, Koch 1974, Armstrong and McGehee 1976, Holt 1984, Tilman 1994, Amarasekare 2003). Extensive evidence exists that structurally complex physical habitats favour increased species diversity, by providing niches and diverse ways of exploiting environmental resources (MacArthur and MacArthur 1961). Yet, many ecosystems with limited abiotic heterogeneity also host a high number of species. Thus, despite the importance of heterogeneity in space and time for species coexistence, we still lack understanding of how species can coexist in environments where underlying abiotic heterogeneity is low.

In recent decades, there has been increasing evidence that strong interactions between organisms and their environment can create environmental heterogeneity, even under uniform, homogeneous conditions, through the process called *spatial self-organization* (Solé and Bascompte 2006, Rietkerk and Van de Koppel 2008). Self-organization processes can generate spatial patterns in ecosystems, through the interaction between local positive and large-scale negative feedbacks (Rietkerk and Van de Koppel 2008). Examples range from vegetation patches alternating with bare soil areas in arid ecosystems (Rietkerk et al. 2002), tree patterns in Siberian peatlands (Eppinga et al. 2008) to diatoms in homogeneous tidal flats (Weerman et al. 2010). Self-organized patterns can cause strong variability in abiotic conditions in their surroundings. By modifying the abiotic environment, self-organizing species can promote

favourable conditions leading to a positive feedback on their own growth (Wilson and Agnew 1992, Rietkerk and Van de Koppel 2008, Kéfi et al. 2016).

Several studies have also focused on the importance of positive interactions that benefit individuals of different species, i.e. interspecific facilitation (Bertness and Callaway 1994, Pugnaire et al. 1996, Callaway and Walker 1997, Brooker et al. 2008). For instance, facilitator species can reduce environmental stress, increasing the realized niche of other species and allowing them to occupy environments that they would normally not inhabit (Bruno et al. 2003, Callaway 2007). Facilitation is in essence based on the same mechanism as self-organization, involving a positive interaction that improves environmental conditions and enhances growth or survival. However, facilitative interactions between two species are mostly considered at a relative local scale, within a tussock or patch of the facilitator species, for instance through "nurse plant effects" in relation to herbivory or drought (Callaway 1995, Padilla and Pugnaire 2006). Instead, studies of self-organization typically focus on a single species at a landscape setting, analysing both scale-dependent effects of local facilitation and large-scale competition (Rietkerk and Van de Koppel 2008, van Wesenbeeck et al. 2008, Schoelynck et al. 2012). Therefore, as the link between self-organization and interspecific facilitation remains unclear, we pose the question whether self-organized pattern formation can create a 'landscape of facilitation'.

In lotic aquatic ecosystems, self-organized patchiness has been found to occur in submerged aquatic vegetation due to scale-dependent feedbacks between plant growth, water flow and sedimentation processes (Schoelynck et al. 2012, Schoelynck et al. 2013). Submerged macrophytes often grow as well-defined, streamlined stands composed of either a single species, or a mixture of species. Macrophytes act as ecosystem engineers (Jones et al. 1994), slowing down the water flow within the patches and promoting sediment deposition (Sand-Jensen and Mebus 1996, Sand-Jensen 1998, Wharton et al. 2006), which creates a local positive

feedback on their own growth and survival. At the same time, flow velocities increase around the patches, creating a large-scale negative feedback on plant growth due to the increased mechanical stress (Puijalon et al. 2011, Schoelynck et al. 2012). In lowland rivers, aquatic macrophytes with different morphologies increase habitat heterogeneity beyond that promoted by hydrodynamic and geomorphological processes alone (Kemp et al. 2000, Gurnell et al. 2006). Despite being suggested by previous observational studies (Jones 1955, Haslam 1978), the consequences of such plant-driven heterogeneity for interspecific interactions have not yet been explored.

We investigated whether self-organized pattern formation in aquatic vegetation promotes the coexistence of different macrophyte species in lotic communities, by generating heterogeneous hydrodynamic conditions and hence creating a 'landscape of facilitation'. First, to demonstrate self-organized pattern formation by the aquatic macrophyte *Callitriche platycarpa* Kütz (various-leaved water starwort), we constructed a spatially explicit mathematical model based on the interaction between plant growth and hydrodynamics. Secondly, we investigated whether such self-organized spatial heterogeneity could promote species coexistence, by modelling the interaction between the pattern-forming species (i.e., facilitator) and two species (i.e., beneficiaries) with different resistance to hydrodynamic stress. Thirdly, to show self-organization and spatial association among species in the field, we compared the model-predicted spatial distribution patterns against field observations on the spatial distribution of two hypothesized beneficiary species (lesser water parsnip, *Berula erecta* (Huds.) Coville and opposite-leaved pondweed, *Groenlandia densa* (L.) Fourr.) around *Callitriche*. Finally, to show that such spatial association provides facilitative interactions, we carried out field transplantations of the two beneficiary species in different locations around patches of the facilitator *Callitriche* as well as on bare sediment, and we investigated if their growth rate, reproduction, and survival correlated with changes in hydrodynamic conditions

created by *Callitriche* patches. Our results suggest that species coexistence in streams is promoted by a biophysical feedback process that creates a landscape of facilitation where multiple new niches emerge for species adapted to a wide range of conditions.

2 Materials and methods

2.1 A model of pattern formation for submerged aquatic macrophytes

Model description

To study the emergence of self-organized patterns in aquatic macrophytes and the potential consequences for species coexistence, we constructed a spatially-explicit mathematical model based on the feedback between vegetation and water flow. The model consists of a set of partial differential equations, where two equations describe the dynamics of plant biomass for the facilitator species *f* (P_f) and for its beneficiary species *b* (P_b), and where water velocity in the streamwise and spanwise directions (u and v), and water depth (h) are described using the shallow water equations (Vreugdenhil 1989).

The rate of change of plant biomass per species in each grid cell can be expressed as:

$$\frac{\partial P_i}{\partial t} = r_i P_i \left(1 - \frac{P_i + \alpha_{ij} P_j}{k_i}\right) \frac{A}{A+S} - m P_i \frac{F}{P_i + F} - m_{Wi} P_i |\boldsymbol{u}| + D_i \Delta P_i \qquad \textbf{(1)}$$

Where $i = f$ and $j = b$ for the equation of the facilitator (pattern-forming) species, and vice versa for a beneficiary (non-pattern forming) species. Here plant growth is described using the logistic growth equation, where r_i is the intrinsic growth rate of the plants and k_i is the plant carrying capacity. Competitive interactions between P_f and P_b are accounted for using the competitive Lotka-Volterra equations, with the term α_{ij} representing the effect P_j has on P_i. Plant growth rate r_i is reduced when sediment accumulation within the plants increases towards its maximum value A; this represents a negative feedback on plant growth due to sediment accumulation and organic matter content becoming high enough to be toxic for the plants

(Barko and Smart (1983); Sofia Licci, personal communication). S is the sediment level (m). Plant mortality m is assumed to decrease with increasing plant density because of a reduction of flow stress in dense vegetation. This is represented by the term $F/(P_i + F)$, where F is an intraspecific facilitation term. Plant mortality caused by water flow stress is modelled as the product of the mortality constant m_{Wi} and net water speed $|\boldsymbol{u}| = \sqrt{(u^2 + v^2)}$ (m s^{-1}) due to plant breakage or uprooting at higher velocities (where u and v are water velocities in the streamwise and spanwise directions). Field sampling on clonal dispersal traits for the aquatic plant species *Berula erecta* and *Groenlandia densa* revealed that plant lateral expansion through vegetative reproduction could be described by a random walk (see Appendix S1: Figure S1). Therefore, we apply a diffusion approximation and use these data to parameterize different diffusion constants D_j for the beneficiary species (Holmes et al. 1994). Clonal dispersal traits for the hypothesized facilitator species *Callitriche platycarpa* could not be estimated based on field sampling, due to the complex morphology of this species. Therefore, the diffusion constant D_i for the facilitator species was given an estimate value.

Changes in sediment level are described as:

$$\frac{\partial S}{\partial t} = S_{in} - E_{max}\frac{K_S}{K_S + P_i}S|\boldsymbol{u}| - |\boldsymbol{u}|\nabla S + D_S\Delta S \qquad \textbf{(2)}$$

where S_{in} is the sediment deposition rate (m t^{-1}), E_{max} is the maximal erosion rate of sediment (t^{-1}) and K_S represents the effects of plants in promoting sediment deposition. The term $|\boldsymbol{u}|\nabla S$ represents the advective flux of sediment over the bottom (i.e., as fluid mud) in any horizontal dimension, and D_S represents the horizontal dispersion rate of sediment, mainly due to flow heterogeneity, and to a lesser extent processes such as bioturbation, which is modelled with a diffusion approximation.

Water flow is modelled using depth-averaged shallow water equations in non-conservative form (Vreugdenhil 1989), to determine water depth and its speed in both x and y directions (see

Appendix S2 for the complete set of equations and description of the variables). The effects of bed and vegetative roughness on flow velocity are represented by determining hydrodynamic roughness characteristics for each cover type separately using the Chézy coefficient, following the approach of Straatsma and Baptist (2008) and Verschoren et al. (2016).

Within the unvegetated cells of the simulated grid, the Chézy roughness of the bed (C_b) is calculated using Manning's roughness coefficient through the following relation:

$$C_b = \frac{1}{n} h^{1/6} \quad \textbf{(3)}$$

where n is Manning's roughness coefficient for an unvegetated gravel bed channel (s/[$m^{1/3}$]) and h is water depth (m).

For each grid cell occupied by submerged vegetation, C_d is calculated using of the equation of Baptist et al. (2007) and slightly modified by Verschoren et al. (2016) to account for reconfiguration of flexible submerged macrophytes, to express vegetation resistance as:

$$C_d = \sqrt{\frac{1}{C_b^{-2} + (2g)^{-1} D_c A_w}} + \frac{\sqrt{g}}{k_v} \ln \frac{h}{H_v} \quad \textbf{(4)}$$

where C_b is the Chézy roughness of the bed, g is acceleration due to gravity (9.81 m s^{-2}), D_c is a species-dependent drag coefficient, A_w is the specific plant surface area (total wetted vertical surface area of the vegetation per unit horizontal surface area of the river (Sand-Jensen 2003, Verschoren et al. 2016)), directly related to plant biomass P_i, k_v is the Von Kármàn constant (0.41), and H_v is the deflected vegetation height (m). Deflected vegetation height varies as a function of incoming flow velocity, due to the high flexibility of submerged aquatic vegetation and reconfiguration at higher stream velocities (Sand-Jensen 2003, Schoelynck et al. 2013). Following the approach of Verschoren et al. (2016), H_v is calculated within each vegetated grid cell as the product of shoot length L (m) and the sine of the bending angle α (degrees), using an empirical relationship between bending angle and incoming current velocity based on flume experiments performed on single shoots of flexible aquatic macrophytes ($\alpha = 15.5 *$

$|\boldsymbol{u}|^{-0.38}$) (Bal et al. 2011). **Table 1** provides an overview of the parameter values used, their interpretations, units and sources.

Model analysis: simulation of species coexistence patterns

To investigate whether spatial pattern formation could promote species coexistence through the creation of spatial heterogeneity in hydrodynamic conditions, we modelled the interaction between the pattern-forming species (P_f, facilitator) and two non-pattern forming species (P_b, beneficiary species). In the first model, we considered the interaction between P_f and a beneficiary species P_{b1} characterized by low resistance to hydrodynamic stress (= high mortality constant m_{Wi}; **Table 1**). In the second model, we considered the interaction between P_f and a second beneficiary species P_{b2} characterized by higher resistance to hydrodynamic stress (= low mortality constant m_{Wi}), but lower growth rate and lower dispersal ability. We modelled the pairwise interactions between the facilitator and each beneficiary separately instead of with a full three-species model. This choice was made to focus on the mechanisms and patterns allowing the coexistence of single beneficiary species with the self-organizing species, instead of studying the coexistence patterns of a whole community. Hence, we focused on studying a self-organized landscape with spatial facilitation, rather than exploring all possible modes of coexistence. The models were analysed by simulating the spatial development of vegetation after random seeding (increasing biomass to 1 in randomly chosen cells) on a spatial grid of 300 x 60 cells, corresponding to a river stretch of 25 m x 5 m. We investigated vegetation development with two-dimensional numerical simulations using the central difference scheme on the finite difference equations. The simulated area consisted of a straight channel with rectangular cross-sectional shape and initial bed slope of 0.03 m m^{-1}. Simulations were started by specifying an initial value of inflowing water speed for the streamwise water flow in the x direction and assuming constant flux. The model was

implemented in Matlab (version 2016b, The MathWorks, Inc.). Simulations were run for 500 time steps, in abstract units due to our non-dimensional description of plant growth.

To test the regularity of the predicted spatial patterns, we analysed the resulting distribution patterns of P_f through spatial autocorrelation. To test the spatial dependence between the beneficiary species P_b and P_f, we used spatial cross-correlation. Both auto- and cross-correlation analyses were performed by calculating Moran's I in the 'ncf' package in R (Bjornstad, 2015). To test for self-organization and spatial association among species in the field, we then compared the auto- and cross-correlation functions from the predicted species distribution patterns of coexistence with field observations on the spatial distribution of *Groenlandia* and *Berula* around *Callitriche* (see paragraph 2.2).

To further explore the implications of self-organization for species coexistence, as opposed to homogeneous environments, we compared the spatial model described above to a simplified, homogeneous (non-spatial) version of the model based on Eq. 1:

$$\frac{dP_i}{dt} = r_i P_i \left(1 - \frac{P_i + \alpha_{ij} P_j}{k_i}\right) - m_{Wi} P_i |\boldsymbol{u}| \qquad \textbf{(5)}$$

Where $i = f$ and $j = b$ for the equation of the facilitator species, and vice versa for a beneficiary species. We used the model to explore the realized niche of each species along the hydrological gradient, under homogeneous (non-spatial) conditions (that is, without self-organization). This simplified version of the model does not account for spatial effects of sedimentation or velocity and intraspecific facilitation. For each imposed flow velocity U_{in} ($|\boldsymbol{u}|$ in Eq. 5), we explored the conditions under which the model predicted either stable coexistence, unstable coexistence or competitive exclusion between the facilitator and beneficiary species (based on the species isoclines of zero growth), as a result of their stress resistance and competitive abilities. Moreover, to show the hydrodynamic heterogeneity generated by the self-organization process and the species hydrological niches predicted in the spatial model, we investigated the frequency distribution of flow velocities within vegetated and unvegetated cells in the spatial

model. The comparison between the two models provided insight and understanding of the mechanisms underlying species coexistence in space.

2.2 Field observation of species coexistence patterns through aerial photographs

To test for significant spatial association of species around self-organized patterns in the field, we examined the distribution of two potential beneficiary species (*Groenlandia* and *Berula*) around the hypothesized facilitator species (*Callitriche*). Submerged macrophytes often grow as well-defined stands composed of a single species or a mixture of species (**Figure 1A**); the patches tend to merge into a more homogeneous cover where streams have low flow velocities sustained over time (**Figure 1B**), while distinct streamlined patches are usually found in streams with sustained periods of moderate to high flow velocities (**Figure 1C**). Vegetation distribution was mapped in two reaches of 100 m in length, through low-altitude aerial photographs. The channels are located along the Rhône River (France), near Serrières-de-Briord (45.815311 ° N, 5.427477 ° E) and Flévieu (45.766738 ° N, 5.479622 ° E) (see Appendix S3: Figure S1 for the location of the study sites). The first reach was mainly colonized by *Callitriche* and *Groenlandia*, with few patches of other macrophyte species, while the second reach was colonized only by *Callitriche* and *Berula*. Aerial pictures of the streambed were taken with a digital camera mounted on a pole at about 2 m height that was moved in the upstream direction along the stretch. Aerial pictures were collected at times of day when the sun was at its highest point, and in the few hours before and after it (between 10:00 and 15:00 hours), to minimize glare. Pictures were collected with a slight overlap and afterwards mosaicked using image processing software (Adobe Photoshop CC 2015). Patches of different species were identified and delineated as shown in Figure 1A; afterwards, pixels where the species was absent were given a value of 0 and pixels where the species was present were given the value of its blue channel in the RGB image, since the intensity of this channel was the one most closely related to differences in plant biomass (evaluated by visual inspection). This

allowed us to obtain different raster maps of macrophyte distribution, one for each of the species considered in the study (non-target species were not included in the analysis). The resulting macrophyte maps were analysed through spatial autocorrelation (to test the distribution of the potential facilitator species) and cross-correlation (to test the spatial dependence between the facilitator and each of the potential beneficiary species), by calculating Moran's *I*. The sample size of our field observations was constrained by the time-intensive nature of our image collection method. Field studies of this nature are often constrained in terms of sample size but can provide valuable insights even without replication (Colegrave and Ruxton 2017). By integrating multiple approaches, the aim of our study was to provide a 'proof of principle' for the mechanisms underlying self-organization and species coexistence in space. Furthermore, the field study in a simplified channel provides a valuable starting point for more observations with different aquatic species and in different stream types. Throughout this paper, the term wake is used to indicate a region of reduced velocity directly downstream from a vegetation patch, i.e. where the flow is laterally uniform and slower than the flow around the patch (Zong and Nepf 2012, Liu and Nepf 2016).

2.3 Testing for positive interactions through a field transplantation experiment

To test for the presence of positive interactions between the hypothesized facilitator *C. platycarpa* and the two hypothesized beneficiary species living in its surroundings, we performed a field transplantation experiment in an artificial drainage channel with natural colonization by aquatic vegetation. The channel is located along the Upper Rhône River (France), near Serrières-de-Briord (45.810657 ° N, 5.447169 ° E), it is 4.26 km long, uniform in terms of width and water depth, with relatively straight banks. The average width is 8.0 m and the average depth is 0.8 m, rarely exceeding 1.3 m. The channel has a substrate of fine sand (d_{50} = 230.87 µm). Flow velocities are on average 0.25 m s^{-1}, with a discharge of 1.48 ± 0.022 m^3 s^{-1} as measured on 21 August 2014 (averaged over five transects in the study site). The

channel is fed by groundwater supply (see description of the flow conditions in the paragraph after the next one and Appendix S4).

Individuals of the two beneficiary species were collected within the same channel on 11th August 2014 and transplanted in five locations around the facilitator patches. Along the patch central axis, transplants were located 20 cm upstream of the leading edge, in the middle (50% of the patch length) and 20 cm downstream of its rear edge. Next to the patch, transplants were positioned at 20 cm to the left and to the right side of its lateral edges, at 50% of the patch length. As a control, an additional treatment was located on bare sediment areas, as far as possible from the influence of existing patches. Since patch effects can be observed for a distance equal to its length (Sand-Jensen and Mebus 1996, Schoelynck et al. 2012), these transplants were located at a distance of at least twice the length of the nearest patch. Ten transplants per treatment were used for each beneficiary species, with one transplant per position around different *C. platycarpa* patches of average length (~ 1.2 m) and in areas outside the influence of other vegetation. Transplants were single plants attached to a stolon without internodes (shoot height of 22.17 ± 1.98 cm for *B. erecta*, 21.48 ± 1.98 cm for *G. densa*). All field transplantation experiments cause a disturbance to the system. However, this disruption and thus its impact on the subsequent observations and measurements was kept to a minimum by creating a small hole of approximately 8 cm in depth and 2-3 cm in diameter in the sediment using a metal pole, to accommodate the rooting part of each single plant shoot. The hole was refilled with sediment almost immediately, and small cobbles were placed around it to prevent scouring and washout of the planted shoots. We observed a limited release of sediment at the time of planting and the conditions stabilized within two days. Transplant survival was monitored two days, four days, and at weekly intervals after transplantation to test for facilitative effects on plant survival. All transplanted individuals were harvested at the end of the experiment (49 days after transplantation, on 29th September 2014). The duration and

timing of the experiment were designed for a period long enough to enable transplants to grow and reproduce by clonal growth (Puijalon et al. 2008, Schoelynck et al. 2012), and to harvest plants at the end of the growing season, before autumnal decay. No storms took place during the experimental period. The average rainfall during the experiment was 1.12 mm per day, and there was no rainfall in 36 out of 49 days of the experiment (see Appendix S5). Growth rates were calculated in terms of shoot height as $GR_H = (H_2 - H_1)/H_1$, with H_1 and H_2 being the shoot height (cm) on day 1 and day 49 of the experiment. Plant height and biomass are highly correlated for *B. erecta* and *G. densa* (e.g. Puijalon and Bornette (2004), Puijalon et al. (2005), Puijalon and Bornette (2006), and based on our previous sampling measurements in Appendix S6). Growth rate in height can be used as a non-destructive alternative to relative growth rate of biomass (Perez-Harguindeguy et al. 2013). Thus, we chose to assess plant size using plant height to minimize plant manipulation at the transplantation date. Moreover, this approach allowed us to keep transplantation time as brief as possible, which is important to avoid plant deterioration. In our case, the plants were harvested from within the same channel and immediately transplanted at the selected study locations without bringing them back to the laboratory for biomass measurements. Here, the initial transplanted individuals were referred to as "mother ramets". New ramets produced by mother ramets through vegetative reproduction were referred to as "daughter ramets", and stolons and daughter ramets together were defined as "juveniles". Shoot height, number of stolons, total stolon length, spacer length, and number of daughter ramets were measured on the transplants. Afterwards, biomass was separated into mother ramet and juveniles, dried in the oven at 60º for 48 h and weighed to obtain the dry mass of the transplants and the biomass investment in vegetative reproduction.

To characterize the flow velocity encountered by transplants for each treatment, both in the surroundings of *C. platycarpa* patches and on bare sediment, we measured flow velocities in the proximity of each transplant. Flow was measured for 100 s at 1 Hz using an Acoustic

Doppler Velocimeter (ADV; FlowTracker, SonTek) at a water depth of 60% from the water surface, to obtain an estimate of average flow velocity over the water column. The study river was selected for its uniform channel structure (cross-section, water depth) and because it is artificially managed by the Compagnie Nationale du Rhône (CNR), maintaining stable conditions in terms of discharge and water levels all year round. Previous measurements at the study site showed that summer flow velocities were stable over time, and this trend was confirmed in the following summer (see Appendix S4: Figure S1). Thus, flow velocity measurements were taken once during the experimental period to characterize the typical flow conditions in different locations around *Callitriche platycarpa* patches. The relative differences in velocity among treatments were assumed to be reasonably constant over time, despite some fluctuation in discharge. The flow velocities encountered by each transplant were subsequently correlated to their growth rates, survival and traits of vegetative reproduction at the end of the experiment.

One-way ANOVA was applied to test for significant differences in dry biomass of transplants between positions around existing patches. Post-hoc comparisons were performed using a Tukey HSD test. Survival of transplants between treatments was analysed using Kaplan-Meier survival analyses and Mantel-Cox log rank tests with Bonferroni correction. The relationships between flow velocity and height increase, spacer length, daughter ramet dry mass, and between mother and daughter ramet height, were tested with a linear regression model. All statistical analyses were performed in R 3.1.2.

3 Results

3.1 Model simulation of species coexistence patterns

Model simulations showing self-organized pattern formation demonstrated that scale-dependent feedbacks between macrophytes, sedimentation, and hydrodynamics could generate

the patchy vegetation distribution observed in the field (**Figure 2A**). Regular patterns of vegetation, consisting of well-defined high biomass patches alternating with bare sediment with little vegetation, develop at intermediate flow velocities. The patches are streamlined and oriented in the main direction of the flow. Due to a scale-dependent interaction of vegetation with water flow, increased flow resistance locally reduces flow velocities within the vegetation, while water flow is diverted and accelerated between the vegetation patches (arrows in **Figure 2A**). Sedimentation is promoted within the patches, up to a point where high sediment accumulation on the downstream side of the patches limits their further length growth in the streamwise direction. Our model highlights that self-organization processes between vegetation growth and hydrodynamics are a potential explanation for the patchy characteristics of many streams, especially at intermediate flow velocities.

When the pattern forming facilitator species P_f is allowed to interact with the non-pattern forming beneficiary species P_b, coexistence is promoted. A beneficiary species P_{b1} with low resistance to hydrodynamic stress is able to colonize the sheltered, low-flow areas in the wake region downstream of the P_f patches, but is outcompeted within the patches themselves (**Figure 2B**). A beneficiary species P_{b2} with lower growth rate r and higher resistance to hydrodynamic stress can coexist inside and locally around the margins of P_f patches, near the high-flow areas created on the sides (**Figure 2C**). Hence, our model shows that, in hydrodynamically stressful habitats, species with different resistance to flow stress can coexist through different spatial patterns, either in the wake of the patterned facilitator species P_f, or locally inside and along the margins of the dominant patterns. These new niches are created by the hydrodynamic heterogeneity resulting from the self-organization process.

Our model analyses also highlight that the presence and strength of the interactions between facilitator and beneficiary species depend strongly on hydrodynamic conditions. The realized biomass of each species under homogeneous conditions (Eq. 5) shows that changes in

incoming flow velocity determine the shift from dominance of one species, to stable coexistence, to dominance of another species (realized biomass distributions in *light green*, *dark green* and *orange*; **Figure 2D**). At low incoming flow velocity (U_{in}), P_{b1} is the most successful competitor (**Figure 2D**); as flow velocity increases, P_{b1} and P_f can coexist within the range $0.07 \leq U_{in} \leq 0.09$. As incoming flow increases further, P_f becomes the dominant species, until a range where it coexists with P_{b2}. At the highest flow velocities, P_{b2} is the most successful competitor due to its higher resistance to flow stress. Based on the species realized niches along the flow velocity gradient, our model analysis also shows that in a spatial model for a given U_{in}, a uniformly distributed P_f would attenuate incoming flow velocity U_{in} to a single realized velocity U_e that would be more favourable for its growth. This flow velocity falls in the range where P_f is predicted to be the only dominant species (**Figure 2D**). Instead, in a spatial model for the same flow velocity, a self-organizing P_f would separate the incoming flow into areas with low velocity (U_e, inside the patches and in their wake) and areas with high velocity (U_e, next to the patches), thus promoting coexistence and diversity by creating a much wider range of hydrodynamic conditions that provide the niches where each species can be dominant (**Figure 2D-E**).

Testing for hydrodynamic heterogeneity under self-organization highlights the very wide range of hydrological niches created by this process in the spatial model (**Figure 2E**). The frequency distribution of flow velocities over the simulated domain shows that self-organization creates a much wider range of hydrodynamic conditions, compared to homogeneous environments. Self-organized patterning leads to a bimodal distribution of flow velocities, with a low-flow peak in vegetated areas, and a high-flow peak in unvegetated areas between plant patches (frequency distributions in *dark green* and *blue*; **Figure 2E**). The self-organizing species therefore provides a spatial flow velocity gradient: low stress areas where less resistant species are more successful, and higher stress areas where more resistant species

are dominant. Such hydrodynamic heterogeneity promotes coexistence by allowing all outcomes of species interactions to occur in space. Depending on the incoming flow velocity U_{in} set at the beginning of the simulation, and on the species included in the model, the extent of the flow attenuation within the patches and acceleration around them (i.e. the ranges of realized velocity U_e) might be different (**Figure 2E)**. Our model highlights that, under self-organization, beneficiary species can persist in environments they would not normally inhabit based on average flow conditions. Therefore, facilitation expands the niches of the beneficiary species and allows them to withstand stronger hydrodynamic stress levels.

3.2 Comparison between simulated and observed species coexistence patterns

Spatial autocorrelation analysis to test for self-organization in the field shows that the spatial patterns of P_f predicted by our numerical model display significant positive autocorrelation up to 1.5 – 2 m distance, followed by significant negative autocorrelation at a distance up to 3 – 3.5 m (**Figure 3A** and **Figure 4A**; *black lines* in **Figure 3C** and **Figure 4C**), reflecting a spatial pattern of vegetated patches alternating with open spaces with a wavelength of about 5 meters. High positive autocorrelation corresponds to more similar plant biomass over 1.5 – 2 m distance (plant aggregation into patches), while the significant negative autocorrelation indicates dissimilarity (plants are not present there due to the negative feedback on their growth).

There is a clearly observable agreement between the spatial correlation function from the field patterns of *C. platycarpa* and the results of the autocorrelation analysis on the predicted patterns. Obviously, differences in patch geometry between the model and the real-world patches appear upon visual inspection (Figure 4A-B), as the model only captures a subset of the relevant processes. Yet, the spatial analysis reveals the regularity of the spatial pattern, with plant aggregation on short scales (positive autocorrelation) and over-dispersion (negative autocorrelation) at larger scales. The mean wavelength of the spatial patterns is, however,

different: *C. platycarpa* patches are located every 5 m in the model and 8 m in the field. Autocorrelation analysis of *C. platycarpa* patches from our aerial pictures either showed significant positive autocorrelation up to 2 m distance, followed by significant negative autocorrelation from 3 to 5 m (**Figure 4B**; *black line* in **Figure 4D**), or it showed a directional effect of significant positive autocorrelation up to 6 m distance, but without negative correlation at any distance due to merging of neighbouring patches (**Figure 3B**; *black line* in **Figure 3D**). Hence, in the first case (**Figure 3D**) we found streamlined bands of vegetation distributed in the direction parallel to the main flow direction, with no clear gap between the patches due to their merging. In the second case (**Figure 4D**), we found regular vegetation patches oriented parallel to the main flow direction, at a distance of roughly 8 m from each other.

When a second species P_b is included in our model, the predicted outcome of species interaction is that P_b can coexist in the low-flow areas created in the wake of the patches of the pattern-forming species P_f (**Figure 3A**). Spatial cross-correlation analysis of P_f with P_b indeed shows a significant positive association of the beneficiary species in the wake of existing patches of the facilitator, as shown by the positive peak in the cross-correlation coefficient at around 1.0 m distance from them (*blue line* in **Figure 3C**). Parallel to the main flow direction, this spatial cross-correlation function shows correspondence to the species coexistence patterns found in the field. *Berula erecta* showed a significant positive association in the wake of *C. platycarpa* patches (**Figure 3D**). Our analysis shows the peak of the beneficiary species around the same downstream location in the field (1.5 m; **Figure 3D**) and simulations (1 m; **Figure 3C**). In contrast, the cross-correlation analysis in the direction perpendicular to the main flow reveals a difference in behaviour between the simulated and observed patterns. Field observations show that *Berula* is located along the outer edges of the *Callitriche* patches (*blue line* in **Figure 3F**). This pattern differs from the model results, where the beneficiary species occupies the region immediately downstream of the facilitator patches (**Figure 3E**).

When P_b is used to model a species with higher resistance to flow stress, a different pattern of coexistence is observed: the beneficiary species grows both within the patches and in the open interspaces around the pattern-forming species (**Figure 4A**; *blue line* in **Figure 4C**). This predicted pattern of coexistence is in strong agreement with field observations on coexistence patterns of *Groenlandia densa* and *Callitriche platycarpa*, where *Groenlandia* tended to coexist within and along the margins of *Callitriche* patches (**Figure 4B**; *blue line* in **Figure 4D**). In both cases, the two species are positively associated up to 2 m distance (i.e., where the patches of the patterned species are located), but negatively or non-significantly correlated from 2 to 5 m distance (i.e., where the patterned species is absent due to the negative feedback on its growth). The relationship between *Callitriche* and *Groenlandia* in the direction perpendicular to the flow in the field still shows a pattern of coexistence (**Figure 4F**), as confirmed by the analysis of the model predictions (**Figure 4E**), while also highlighting a shift in the lateral distribution of the two species as *Groenlandia* tends to grow along the margins of *Callitriche* patches.

3.3 Field transplantation: effects on growth, vegetative reproduction and survival

Growth rates:

Our experiments testing for the presence of facilitative interactions showed a positive effect on the growth of both beneficiary species *Berula erecta* and *Groenlandia densa* when located in the wake of *Callitriche platycarpa* patches, compared to bare areas without vegetation. Transplants in locations sheltered by the patches ('Downstream' treatment) showed a significantly higher increase in shoot height compared with transplants on the 'Bare sediment' treatment (t-test, $t = 4.3$, $df = 4.387$, $p = 0.02$ for *Berula*; $t = 5.5$, $df = 1.839$, $p = 0.04$ for *Groenlandia*). The intensity of this effect was correlated with the reduction in flow velocity created by the facilitator species ($r^2 = 0.96$, $p = 0.0004$ for *Berula*, $r^2 = 0.82$, $p = 0.03$ for *Groenlandia*; **Figure 5**).

Vegetative reproduction:

No difference in dry mass invested in vegetative reproduction was found for either species between transplant positions (**Figure 6C, F**). Dry mass investment was not correlated with incoming flow velocity for *B. erecta* ($r^2 = 0.0168$, $p > 0.05$) or for *G. densa* ($r^2 = 0.48$, $p = 0.19$). A significant negative correlation was found between the average spacer length in the transplants and incoming flow velocity for *B. erecta* ($r^2 = 0.84$, $p = 0.01$; **Figure 6A**). The correlation was not significant for *G. densa* ($r^2 = 0.64$, $p = 0.19$; **Figure 6D**). A significant positive correlation was found between the height of the mother ramet transplant and their average daughter ramet height for both *B. erecta* ($r^2 = 0.65$, $p = 0.05$) and *G. densa* ($r^2 = 0.85$, $p = 0.02$) (**Figure 6B, E**).

Transplant survival:

Survival of transplanted individuals showed no significant relationship with local flow velocity up to 0.3 m s^{-1} ($r^2 = 0.20$, $p = 0.37$ for *B. erecta*; $r^2 = 0.44$, $p = 0.15$ for *G. densa*). However, survival curve analysis revealed significant differences in survival between treatments (Kaplan-Meier Mantel Cox, *Berula erecta*: $\chi^2 = 16.1$, $p = 0.00648$; *Groenlandia densa*: $\chi^2 = 11.9$, $p = 0.036$). Pairwise comparisons between treatments revealed that survival in the middle of the patch was significantly lower than on bare sediment for *B. erecta*, but not for *G. densa* ($p = 0.033$ and $p = 0.4205$ respectively, adjusted after Bonferroni correction; **Table 2**).

4 Discussion

In a combined mathematical and empirical study, we reveal that bio-physical feedbacks between in-stream submerged plants and streamflow can generate spatial heterogeneity in hydrodynamic conditions that create new niches, promoting species coexistence in streams. Central to this landscape of facilitation is spatial self-organization of submerged aquatic

vegetation by means of deflection of water flow by the facilitator species, *Callitriche platycarpa*, which generates a patterned landscape of *Callitriche* patches. Our mathematical model shows that (1) the hydrodynamic heterogeneity results from the self-organization process and (2) it promotes coexistence by creating new niches for species that are adapted to a wider variety of environmental conditions. Species distribution patterns from our numerical model showed similarities with the spatial aggregation of macrophyte species around *Callitriche platycarpa* patches observed in the field at the reach scale. A field transplantation experiment revealed that species coexistence results from a positive interaction due to stress amelioration, as the growth of these beneficiary species was facilitated by the hydrodynamic stress reduction mediated by *Callitriche* patches. Moreover, the effects of self-organized pattern formation on species interactions go beyond the spatial structure of the vegetation community. By affecting clonal growth traits, *Callitriche* patches also affect the density of the patches of other species, and therefore the spatial organization and appearance of vegetation patterns for the beneficiary species. Our study highlights that species coexistence in streams is, in part, explained by a biophysical feedback process that creates a heterogeneous landscape offering facilitative effects.

Landscapes of facilitation through self-organized patchiness

Current theory largely ignores the spatial dimension when considering facilitative effects between species (Callaway (2007), Smit et al. (2007), Cavieres et al. (2014); but see van de Koppel et al. (2006), van de Koppel et al. (2015) for a review). Facilitative interactions are for the most part considered within the tussocks or patches of the facilitator species, and to date experiments have focused on this local scale, as beneficiary species are mainly considered to be living inside the facilitator patches (e.g. nurse plants in drylands; Callaway and Walker (1997), Badano and Cavieres (2006); but see Pescador et al. (2014)). Through this approach, many studies have shown the importance of facilitation but few have looked at its spatial

variability. Here, we reveal that in self-organized ecosystems, facilitative interactions are far from being homogeneous in space, and display strong spatial heterogeneity due to the balance between positive and negative feedbacks. The self-organizing process leads to spatial separation of competition and facilitation, with opposite effects balancing throughout the landscape. Similar long-distance effects through modification of physical forcing by ecosystem engineers have also been observed in other systems, such as mussel beds on tidal flats (Donadi et al. 2013) or between adjacent tropical ecosystems at the landscape scale (Gillis et al. 2014). The heterogeneity of facilitation and its spatial effects are important processes that have been identified in previous studies (Bruno 2000, Bruno and Kennedy 2000, van de Koppel et al. 2006), although not in the context of self-organized ecosystems. Hence, we show that self-organization acts as a strong structuring force of community composition and distribution by creating spatial variability in environmental conditions, leading to facilitative interactions at different spatial scales.

Our results emphasize that by triggering a self-organized pattern, a single engineering species may create a 'landscape of facilitation', where multiple mechanisms of coexistence co-occur due to the conditions created by the self-organized process. The conditions include: low stress – high competition inside the patch; low stress – low competition downstream of the patch; and high stress – low competition next to the patch. As the facilitative effects described here extend over longer distances, species with higher resistance to stress can locally colonize the open interspaces around the patches, exploiting the new niches created by the negative feedback without being exposed to high competition; less tolerant species can grow at a certain distance from the patch, where the positive feedback of stress reduction is still present, but there is no negative effect of competition.

The comparisons between field vegetation patterns and model outputs highlight areas for further detailed experiments and model improvement. Our model is minimalistic and does not

capture all of the relevant processes that occur in real streams. For instance, as the vegetation density increases, canopy-scale turbulence can lead to higher sediment resuspension within the vegetation (Yang et al. 2016), creating patterns of enhanced or diminished turbulence and sediment deposition in different locations. Moreover, the scaling of stem-scale and patch-scale turbulent wakes can limit the deposition of fine material downstream of a patch (Chen et al. 2012, Liu and Nepf 2016). These findings suggest that *Berula erecta* might occupy optimal zones where sediment can be deposited, downstream of the termination of the turbulent wake structure and along the outer edges of *Callitriche* patches. Consistent with this, earlier studies by Sand-Jensen (1998) observed turbulent eddies and sediment erosion at the rear end of macrophyte patches of species with an overhanging canopy. These complex patterns in turbulence and sediment deposition are interesting possible extensions of the model that will provide an even more elaborate mechanistic basis for habitat and species diversity in streams.

Although our model depicts a simplification of the complex hydrodynamic-vegetation interactions, the comparison between the predicted and observed spatial patterns suggests that the spatial distribution of *Berula erecta* is similar to that of a beneficiary species with lower resistance to hydrodynamic stress, while *Groenlandia densa* exhibits greater behavioural similarity to species with higher resistance to stress. The differences in stress resistance between the two species are also supported by our transplantation experiments. For *Groenlandia densa,* we found a steeper slope and larger y-intercept of the negative relationship between flow velocity and growth rate, compared to *Berula erecta* (Figure 5). As the regression line for *Groenlandia* is located above the line for *Berula* across the whole range of flow velocities in our experiment, the former appears to perform consistently better in response to flow stress. Survival results for *Berula erecta* showed significantly higher mortality within the patch than in the other treatments, suggesting that short-range competition for light prevails in that location. However, while we found a facilitative effect in terms of growth rates of the initial

transplanted individuals, we found no effect on the biomass they invested in vegetative reproduction (through clonal growth). This observation is consistent with the ability of *B. erecta* to maintain its investment in vegetative growth and produce a more compact clonal growth form, despite the increased flow stress (Puijalon et al. 2005, Puijalon and Bornette 2006). Therefore, self-organization processes allow the coexistence of species with a wide range of growth strategies and sensitivity to stress.

Effects of self-organization on species coexistence

The process of pattern formation allows species to coexist, even if the number of resources on which they grow would predict competitive exclusion (Gause 1932). The results from our study on submerged macrophytes in streams are in accordance with the only known previous theoretical studies of pattern formation and species coexistence albeit on arid savannas (Gilad et al. 2004, Baudena and Rietkerk 2013, Nathan et al. 2013). However, while these studies found coexistence of two species within the same spatial pattern (i.e. overlapping patches), we found that self-organization effects act both locally and at distance beyond the limits of the facilitator canopy (in the order of a few meters of the river reach in our study). Hence, self-organization can provide a potential explanation for the high biodiversity observed in many natural communities, despite theoretical predictions of low species coexistence.

Self-organization differs from ecosystem engineering and local facilitation between species in important ways. While ecosystem engineering creates a local positive feedback, self-organized patchiness also results from both a positive and a strong negative feedback. This negative feedback has a two-fold role. First, it prevents the facilitating species from dominating the entire habitat. Second, it changes environmental conditions within the inter-patch spaces, allowing for the coexistence of a wide range of species as compared to the original, more homogeneous habitat. Therefore, the emergence of self-organized patterns produces distinct

spatial signatures in plant community structure that might be discerned from local facilitation effects.

The creation of new niches and the effects on biodiversity arising from facilitation can benefit both plant and animal species. For instance, fish can use both the shelter provided by plants as protection from predation, and the high-flow areas around patches as spawning and feeding grounds (Kozarek et al. 2010, Marjoribanks et al. 2016); and suspension-feeding invertebrates (e.g. blackfly larvae) can grow on the edge of submerged macrophyte patches, such as *Ranunculus* sp. where higher current velocities increase the flux of resources (Wharton et al. 2006). Thus, spatial self-organization has the ability to affect many species within stream communities at different trophic levels.

Relevance beyond stream ecosystems

The importance of pattern formation in promoting species coexistence is likely to be relevant for a wide range of self-organized ecosystems. In many of these systems, at least one habitat-forming species provides structure for an entire community. For example, periodic vegetation patterns in arid or semi-arid systems create different levels of edaphic and climatic stress for other species (Couteron 2001, Rietkerk et al. 2002). In coastal environments, mussel beds on relatively homogeneous intertidal flats reduce wave stress and increase habitat structural complexity and species richness (Gutiérrez et al. 2003, van de Koppel et al. 2005, van de Koppel et al. 2008, Donadi et al. 2013, Christianen et al. 2016) and salt marsh plants create different spatial patterns of sediment deposition, salinity and redox conditions (Howes et al. 1980, Callaway 1994, Hacker and Bertness 1999). Thus, as self-organized patterns emerge as a widespread phenomenon, landscapes of facilitation which enhance species coexistence and biodiversity are likely to be of similar ecological importance.

In ecosystems with limited underlying heterogeneity in abiotic conditions, self-organization acts as a powerful structuring force of community composition and distribution. These findings

can be used to inform ecological restoration projects, which aim to maximize biodiversity through the preservation or re-introduction of self-organized species. Exploring the implications of species coexistence promoted by self-organization on food web structure is also an interesting topic for future studies. Understanding of the intricate way in which competition and facilitation interact in many ecosystems is key to successful management of their biodiversity.

Acknowledgements This work was supported by the Research Executive Agency, through the Seventh Framework Programme of the European Union, Support for Training and Career Development of Researchers (Marie Curie - FP7-PEOPLE-2012-ITN), which funded the Initial Training Network (ITN) HYTECH 'Hydrodynamic Transport in Ecologically Critical Heterogeneous Interfaces', N.316546. We thank Vanessa Gardette, Bruno Pyronain and Youssouf Sy for field and laboratory assistance. We thank the CNR (Compagnie Nationale du Rhône) for providing access to field sites.

5 Literature cited

Amarasekare, P. 2003. Competitive coexistence in spatially structured environments: a synthesis. Ecology Letters **6**:1109-1122.

Arcement, G. J., and V. R. Schneider. 1989. Guide for selecting Manning's roughness coefficients for natural channels and flood plains. Pages 1-38. US Government Printing Office Washington, DC, USA.

Armstrong, R. A., and R. McGehee. 1976. Coexistence of species competing for shared resources. Theoretical Population Biology **9**:317-328.

Badano, E. I., and L. A. Cavieres. 2006. Impacts of ecosystem engineers on community attributes: effects of cushion plants at different elevations of the Chilean Andes. Diversity and Distributions **12**:388-396.

Bal, K. D., T. J. Bouma, K. Buis, E. Struyf, S. Jonas, H. Backx, and P. Meire. 2011. Trade-off between drag reduction and light interception of macrophytes: comparing five aquatic plants with contrasting morphology. Functional Ecology **25**:1197-1205.

Baptist, M., V. Babovic, J. Rodríguez Uthurburu, M. Keijzer, R. Uittenbogaard, A. Mynett, and A. Verwey. 2007. On inducing equations for vegetation resistance. Journal of Hydraulic Research **45**:435-450.

Barko, J., and R. Smart. 1983. Effects of organic matter additions to sediment on the growth of aquatic plants. The journal of Ecology:161-175.

Baudena, M., and M. Rietkerk. 2013. Complexity and coexistence in a simple spatial model for arid savanna ecosystems. Theoretical Ecology **6**:131-141.

Bertness, M. D., and R. Callaway. 1994. Positive interactions in communities. Trends in Ecology & Evolution **9**:191-193.

Brooker, R. W., F. T. Maestre, R. M. Callaway, C. L. Lortie, L. A. Cavieres, G. Kunstler, P. Liancourt, K. Tielbörger, J. M. Travis, and F. Anthelme. 2008. Facilitation in plant communities: the past, the present, and the future. Journal of Ecology **96**:18-34.

Bruno, J. F. 2000. Facilitation of cobble beach plant communities through habitat modification by Spartina alterniflora. Ecology **81**:1179-1192.

Bruno, J. F., and C. W. Kennedy. 2000. Patch-size dependent habitat modification and facilitation on New England cobble beaches by Spartina alterniflora. Oecologia **122**:98-108.

Bruno, J. F., J. J. Stachowicz, and M. D. Bertness. 2003. Inclusion of facilitation into ecological theory. Trends in Ecology & Evolution **18**:119-125.

Callaway, R. M. 1994. Facilitative and interfering effects of *Arthrocnemum subterminale* on winter annuals. Ecology **75**:681-686.

Callaway, R. M. 1995. Positive interactions among plants. The Botanical Review **61**:306-349.

Callaway, R. M. 2007. Direct Mechanisms for Facilitation. Pages 15-116 Positive Interactions and Interdependence in Plant Communities. Springer Netherlands, Dordrecht.

Callaway, R. M., and L. R. Walker. 1997. Competition and facilitation: a synthetic approach to interactions in plant communities. Ecology **78**:1958-1965.

Cavieres, L. A., R. W. Brooker, B. J. Butterfield, B. J. Cook, Z. Kikvidze, C. J. Lortie, R. Michalet, F. I. Pugnaire, C. Schöb, and S. Xiao. 2014. Facilitative plant interactions and climate simultaneously drive alpine plant diversity. Ecology Letters **17**:193-202.

Chen, Z., A. Ortiz, L. Zong, and H. Nepf. 2012. The wake structure behind a porous obstruction and its implications for deposition near a finite patch of emergent vegetation. Water Resources Research **48**.

Christianen, M., T. van der Heide, S. Holthuijsen, K. van der Reijden, A. Borst, and H. Olff. 2016. Biodiversity and food web indicators of community recovery in intertidal shellfish reefs. Biological Conservation. http://dx.doi.org/10.1016/j.biocon.2016.09.028.

Colegrave, N., and G. D. Ruxton. 2017. Using Biological Insight and Pragmatism When Thinking about Pseudoreplication. Trends in Ecology & Evolution.

Couteron, P. 2001. Using spectral analysis to confront distributions of individual species with an overall periodic pattern in semi-arid vegetation. Plant Ecology **156**:229-243.

Donadi, S., T. van der Heide, E. M. van der Zee, J. S. Eklöf, J. v. de Koppel, E. J. Weerman, T. Piersma, H. Olff, and B. K. Eriksson. 2013. Cross-habitat interactions among bivalve species control community structure on intertidal flats. Ecology **94**:489-498.

Eppinga, M. B., M. Rietkerk, W. Borren, E. D. Lapshina, W. Bleuten, and M. J. Wassen. 2008. Regular surface patterning of peatlands: confronting theory with field data. Ecosystems **11**:520-536.

Gause, G. F. 1932. Experimental studies on the struggle for existence. Journal of Experimental Biology **9**:389-402.

Gilad, E., J. von Hardenberg, A. Provenzale, M. Shachak, and E. Meron. 2004. Ecosystem engineers: from pattern formation to habitat creation. Physical Review Letters **93**:098105.

Gillis, L., T. Bouma, C. Jones, M. Van Katwijk, I. Nagelkerken, C. Jeuken, P. Herman, and A. Ziegler. 2014. Potential for landscape-scale positive interactions among tropical marine ecosystems. Marine Ecology Progress Series **503**:289-303.

Gurnell, A., M. Van Oosterhout, B. De Vlieger, and J. Goodson. 2006. Reach-scale interactions between aquatic plants and physical habitat: River Frome, Dorset. River Research and Applications **22**:667-680.

Gutiérrez, J. L., C. G. Jones, D. L. Strayer, and O. O. Iribarne. 2003. Mollusks as ecosystem engineers: the role of shell production in aquatic habitats. Oikos **101**:79-90.

Hacker, S. D., and M. D. Bertness. 1999. Experimental evidence for factors maintaining plant species diversity in a New England salt marsh. Ecology **80**:2064-2073.

Haslam, S. M. 1978. River plants. London.

Holmes, E. E., M. A. Lewis, J. Banks, and R. Veit. 1994. Partial differential equations in ecology: spatial interactions and population dynamics. Ecology **75**:17-29.

Holt, R. D. 1984. Spatial heterogeneity, indirect interactions, and the coexistence of prey species. The American Naturalist **124**:377-406.

Howes, B. L., R. W. Howarth, J. M. Teal, and I. Valiela. 1980. Oxidation-reduction potentials in a salt marsh: spatial patterns and interactions with primary production. Boston University.

Hutchinson, G. E. 1961. The paradox of the plankton. The American Naturalist **95**:137-145.

Jones, C. G., J. H. Lawton, and M. Shachak. 1994. Organisms as ecosystem engineers. Pages 130-147 Ecosystem management. Springer.

Jones, H. 1955. Studies on the Ecology of the River Rheidol: I. Plant Colonization and Permanent Quadrat Records in the Main Stream of the Lower Rheidol. Journal of Ecology **43**:462-476.

Kéfi, S., M. Holmgren, and M. Scheffer. 2016. When can positive interactions cause alternative stable states in ecosystems? Functional Ecology **30**:88-97.

Kemp, J. L., D. M. Harper, and G. A. Crosa. 2000. The habitat-scale ecohydraulics of rivers. Ecological Engineering **16**:17-29.

Koch, A. L. 1974. Competitive coexistence of two predators utilizing the same prey under constant environmental conditions. Journal of Theoretical Biology **44**:387-395.

Kozarek, J., W. Hession, C. Dolloff, and P. Diplas. 2010. Hydraulic complexity metrics for evaluating in-stream brook trout habitat. Journal of Hydraulic Engineering **136**:1067-1076.

Levin, R. 1970. Extinction. Some mathematical problems in biology. American Mathematical Society, Providence, Rhode Island:77-107.

Liu, C., and H. Nepf. 2016. Sediment deposition within and around a finite patch of model vegetation over a range of channel velocity. Water Resources Research **52**:600-612.

MacArthur, R. H., and J. W. MacArthur. 1961. On bird species diversity. Ecology **42**:594-598.

Marjoribanks, T. I., R. J. Hardy, S. N. Lane, and M. J. Tancock. 2016. Patch-scale representation of vegetation within hydraulic models. Earth Surface Processes and Landforms.

Naden, P., P. Rameshwaran, and P. Vienot. 2004. Modelling the influence of instream macrophytes on velocity and turbulence. Pages 1118-1122 *in* Proceedings of the Fifth International Symposium on Ecohydraulics.

Nathan, J., J. von Hardenberg, and E. Meron. 2013. Spatial instabilities untie the exclusion-principle constraint on species coexistence. Journal of Theoretical Biology **335**:198-204.

Padilla, F. M., and F. I. Pugnaire. 2006. The role of nurse plants in the restoration of degraded environments. Frontiers in Ecology and the Environment **4**:196-202.

Perez-Harguindeguy, N., S. Diaz, E. Garnier, S. Lavorel, H. Poorter, P. Jaureguiberry, M. Bret-Harte, W. K. Cornwell, J. M. Craine, and D. E. Gurvich. 2013. New handbook for standardised measurement of plant functional traits worldwide. Australian Journal of botany **61**:167-234.

Pescador, D. S., J. Chacón-Labella, M. Cruz, and A. Escudero. 2014. Maintaining distances with the engineer: patterns of coexistence in plant communities beyond the patch-bare dichotomy. New Phytologist **204**:140-148.

Pugnaire, F. I., P. Haase, and J. Puigdefabregas. 1996. Facilitation between higher plant species in a semiarid environment. Ecology **77**:1420-1426.

Puijalon, S., and G. Bornette. 2004. Morphological variation of two taxonomically distant plant species along a natural flow velocity gradient. New Phytologist **163**:651-660.

Puijalon, S., and G. Bornette. 2006. Phenotypic plasticity and mechanical stress: biomass partitioning and clonal growth of an aquatic plant species. American Journal of Botany **93**:1090-1099.

Puijalon, S., G. Bornette, and P. Sagnes. 2005. Adaptations to increasing hydraulic stress: morphology, hydrodynamics and fitness of two higher aquatic plant species. Journal of Experimental Botany **56**:777-786.

Puijalon, S., T. J. Bouma, C. J. Douady, J. van Groenendael, N. P. Anten, E. Martel, and G. Bornette. 2011. Plant resistance to mechanical stress: evidence of an avoidance–tolerance trade-off. New Phytologist **191**:1141-1149.

Puijalon, S., J. P. Léna, N. Rivière, J. Y. Champagne, J. C. Rostan, and G. Bornette. 2008. Phenotypic plasticity in response to mechanical stress: hydrodynamic performance and fitness of four aquatic plant species. New Phytologist **177**:907-917.

Rietkerk, M., M. C. Boerlijst, F. van Langevelde, R. HilleRisLambers, J. van de Koppel, L. Kumar, H. H. Prins, and A. M. de Roos. 2002. Self-organization of vegetation in arid ecosystems. The American Naturalist **160**:524-530.

Rietkerk, M., and J. Van de Koppel. 2008. Regular pattern formation in real ecosystems. Trends in Ecology & Evolution **23**:169-175.

Sand-Jensen, K. 1998. Influence of submerged macrophytes on sediment composition and near-bed flow in lowland streams. Freshwater Biology **39**:663-679.

Sand-Jensen, K. 2003. Drag and reconfiguration of freshwater macrophytes. Freshwater Biology **48**:271-283.

Sand-Jensen, K., and J. R. Mebus. 1996. Fine-scale patterns of water velocity within macrophyte patches in streams. Oikos:169-180.

Schoelynck, J., T. De Groote, K. Bal, W. Vandenbruwaene, P. Meire, and S. Temmerman. 2012. Self-organised patchiness and scale-dependent bio-geomorphic feedbacks in aquatic river vegetation. Ecography **35**:760-768.

Schoelynck, J., D. Meire, K. Bal, K. Buis, P. Troch, T. Bouma, P. Meire, and S. Temmerman. 2013. Submerged macrophytes avoiding a negative feedback in reaction to hydrodynamic stress. Limnologica-Ecology and Management of Inland Waters **43**:371-380.

Smit, C., C. Vandenberghe, J. Den Ouden, and H. Müller-Schärer. 2007. Nurse plants, tree saplings and grazing pressure: changes in facilitation along a biotic environmental gradient. Oecologia **152**:265-273.

Solé, R. V., and J. Bascompte. 2006. Self-Organization in Complex Ecosystems. Princeton University Press.

Straatsma, M. W., and M. Baptist. 2008. Floodplain roughness parameterization using airborne laser scanning and spectral remote sensing. Remote Sensing of Environment **112**:1062-1080.

Tilman, D. 1994. Competition and biodiversity in spatially structured habitats. Ecology **75**:2-16.

van de Koppel, J., A. H. Altieri, B. R. Silliman, J. F. Bruno, and M. D. Bertness. 2006. Scale-dependent interactions and community structure on cobble beaches. Ecology Letters **9**:45-50.

van de Koppel, J., J. C. Gascoigne, G. Theraulaz, M. Rietkerk, W. M. Mooij, and P. M. Herman. 2008. Experimental evidence for spatial self-organization and its emergent effects in mussel bed ecosystems. Science **322**:739-742.

van de Koppel, J., M. Rietkerk, N. Dankers, and P. M. Herman. 2005. Scale-dependent feedback and regular spatial patterns in young mussel beds. The American Naturalist **165**:E66-E77.

van de Koppel, J., T. van der Heide, A. H. Altieri, B. K. Eriksson, T. J. Bouma, H. Olff, and B. R. Silliman. 2015. Long-distance interactions regulate the structure and resilience of coastal ecosystems. Annual review of marine science **7**:139-158.

van Wesenbeeck, B. K., J. Van De Koppel, P. MJ Herman, and T. J Bouma. 2008. Does scale-dependent feedback explain spatial complexity in salt-marsh ecosystems? Oikos **117**:152-159.

Verschoren, V., D. Meire, J. Schoelynck, K. Buis, K. D. Bal, P. Troch, P. Meire, and S. Temmerman. 2016. Resistance and reconfiguration of natural flexible submerged vegetation in hydrodynamic river modelling. Environmental Fluid Mechanics **16**:245-265.

Vreugdenhil, C. B. 1989. Computational hydraulics: an introduction. Springer Science & Business Media.

Weerman, E. J., J. Van de Koppel, M. B. Eppinga, F. Montserrat, Q. X. Liu, and P. M. Herman. 2010. Spatial Self-Organization on Intertidal Mudflats through Biophysical Stress Divergence. The American Naturalist **176**:E15-E32.

Wharton, G., J. A. Cotton, R. S. Wotton, J. A. Bass, C. M. Heppell, M. Trimmer, I. A. Sanders, and L. L. Warren. 2006. Macrophytes and suspension-feeding invertebrates modify flows and fine sediments in the Frome and Piddle catchments, Dorset (UK). Journal of Hydrology **330**:171-184.

Wilson, J. B., and A. D. Agnew. 1992. Positive-feedback switches in plant communities. Advances in Ecological Research **23**:263-336.

Yang, J., H. Chung, and H. Nepf. 2016. The onset of sediment transport in vegetated channels predicted by turbulent kinetic energy. Geophysical Research Letters **43**.

Zong, L., and H. Nepf. 2012. Vortex development behind a finite porous obstruction in a channel. Journal of Fluid Mechanics **691**:368-391.

Table 1. Symbols, interpretations, values, units and sources used in the model simulations.

Symbol	Interpretation	Value			Unit	Source
		P_f	P_{b1}	P_{b2}		
r_i	Intrinsic growth rate species *i*	1	1	0.5	t^{-1}	Estimated
k_i	Carrying capacity of species *i*	200	200	200	g m^{-2} dry biomass	Sand-Jensen and Mebus (1996)
m_{Wi}	Plant mortality constant due to hydrodynamic stress	9	8	3	Dimensionless	Estimated
D_i	Diffusion constant of species *i*	0.00045	0.00025	0.00015	m^2 t^{-1}	Estimated
m_i	Mortality of species *i*	0.02	0.02	0.02	Dimensionless	Estimated
α_{fb}	Interaction coefficient of P_b on P_f		2	0.5	Dimensionless	Estimated
α_{bf}	Interaction coefficient of P_f on P_b		4	0.1	Dimensionless	Estimated
n	Manning's roughness coefficient for unvegetated gravel bed		0.035		s/[$m^{1/3}$]	Arcement and Schneider (1989)
D_c	Drag coefficient	0.5	0.5	0.5	Dimensionless	Naden et al. (2004)
L	Shoot length	0.5	0.5	0.5	m	Bal et al. (2011)
S_{in}	Sediment deposition rate		0.0012		m t^{-1}	Estimated
E_{max}	Maximal sediment erosion		200		t^{-1}	Estimated
Ki_s	Sediment deposition due to vegetation	0.0005	0.008	0.008		Estimated
D_S	Diffusion constant of sediment		0.01		m^2 t^{-1}	Estimated
A_i	Toxicity feedback of sediment accumulation on plant growth	0.02	0.005	0.008		Estimated

Table 2. Results of Kaplan–Meier Mantel–Cox log-rank test on transplant survival during the field experiment. Differences between treatments (transplant position around *C. platycarpa* patches) were tested against the 'bare sediment' treatment. P-values are adjusted using Bonferroni correction. The sign column indicates whether survival was higher (+), lower (-) or equal (=) to the bare sediment treatment.

Species	Treatment	Log-rank of survival				Sign
		χ^2	d.f.	p-value	adjusted p-value	
Berula erecta	Middle	7.4	1	0.0066	0.0330	-
	Channel	5.1	1	0.0244	0.1220	-
	Downstream	2.3	1	0.1280	0.6400	-
	Upstream	1.2	1	0.2760	1.0000	-
	Bank	0.2	1	0.6860	1.0000	+
Groenlandia densa	Middle	3	1	0.0841	0.4205	-
	Channel	0.2	1	0.6590	1.0000	=
	Downstream	0.1	1	0.7470	1.0000	=
	Upstream	2.4	1	0.1180	0.5900	+
	Bank	0	1	0.8650	1.0000	=

Figure legends

Figure 1. (A) Aerial picture showing the patchy distribution of the macrophyte species *Callitriche platycarpa* (light green patches, outlined in yellow), in the drainage channel of Serrières-de-Briord (France). Other aquatic macrophytes, such as *Groenlandia densa* (dark green vegetation, outlined in light blue), are often found in close proximity to, or within *Callitriche* patches, forming 'mixed' vegetation stands. **(B)** and **(C)** Aerial photographs of vegetation patterns observed in streams with two different values of incoming flow velocity (U, m s^{-1}). In streams with sustained periods of low flow velocities, vegetation patches tend to merge into a more homogeneous cover. In streams with moderate flow velocities, regular and well-defined vegetation patches are found, streamlined in the main current direction. Water flow is from right to left in the pictures.

Figure 2. (A) Spatial patterns of macrophyte distribution in the simulated stream reach. Small spatial heterogeneities lead to the development of regular patterns in the distribution of the facilitator P_f, where dense vegetation patches (*in grey*) alternate with almost bare sediment and low vegetation biomass. Due to a scale-dependent interaction with water flow, flow velocities are locally reduced within the vegetation and accelerated outside (indicated by arrow size and color, from yellow to red). **(B)** Beneficiary species characterized by low resistance to hydrodynamic stress (*light green*) colonize the sheltered, low-flow areas in the wake of the P_f patches (*dark green*), while being outcompeted within the patches themselves. **(C)** Beneficiary species with lower growth rate and higher resistance to hydrodynamic stress (*orange*) can coexist inside and locally around the P_f patches (*dark green*), near the high-flow channels created next to them. **(D)** Realized niches of P_f, P_{b1} and P_{b2} along the hydrodynamic stress gradient in the homogeneous model. Dashed lines indicate the limits between the flow velocity ranges where either one species is dominant, or two species coexist. In a spatial model for a given U_{in}, a uniformly distributed P_f would attenuate incoming flow velocity U_{in} to a single realized velocity U_e. This flow velocity falls in the range where P_f is predicted to be the only dominant species (based on the species realized niches along the flow velocity gradient, in D). Instead, for the same flow velocity, a self-organizing P_f would separate the incoming flow into areas with low velocity (U_e, inside and downstream of the patches) and areas with high velocity (U_e, next to the patches), thus creating a wider range of hydrodynamic conditions that provide the niches where each species can be dominant (in D – E). Parameters used are r_f = 1.19, α_{fb1} = 0.6, α_{b1f} = 1.42, k_{b1} = 390, r_{b1} = 0.94, α_{b2f} = 0.83, k_{b2} = 100. Other parameters as in Table 1. **(E)** Hydrodynamic heterogeneity generated by self-organization in the spatial model: frequency distribution of depth-averaged flow velocities within vegetated (*dark green*) and unvegetated cells (*blue*) of the simulated domain. The two subfigures refer for the two beneficiary species: P_{b1} (top figure) and P_{b2} (bottom figure).

Figure 3. (A) Model simulations of aquatic vegetation development on a 150 x 30 grid for P_f (facilitator) and P_b (beneficiary). **(B)** Field observations of *Callitriche* and *Berula* distribution in a river stretch of 100 m, obtained from aerial pictures. Individual patches can be obscured because they can merge and grow above another, but 7 patches of *Berula* and more than 20 of *Callitriche* were present in the reach. Please note the scale difference compared to the model in (A). Auto- and cross-correlation functions of species distribution patterns from model simulations **(C)** and field observations **(D)** in the direction parallel to the main water flow. Auto- and cross-correlation functions of species distribution patterns from model simulations **(E)** and field observations **(F)** in the direction perpendicular to the main water flow. In C and E, *black lines* are the autocorrelation functions for the simulated spatial patterns of P_f, *blue lines* are the cross-correlation functions between P_f and P_b. In D and F, *black lines* are the

autocorrelation functions for *Callitriche platycarpa*; *blue lines* are the cross-correlation functions between *Callitriche* and *Berula*. Closed dots represent significant values.

Figure 4. (A) Model simulations of aquatic vegetation development on a 150 x 30 grid for P_f (facilitator) and P_b (beneficiary). **(B)** Field observations of *Callitriche* and *Groenlandia* distribution in a river stretch of 100 m, obtained from aerial pictures. Individual patches can be obscured because they can merge and grow above another, but 9 patches of *Groenlandia* and more than 30 of *Callitriche* were present in the reach. Please note the scale difference compared to the model in (A). Auto- and cross-correlation functions of species distribution patterns from model simulations **(C)** and field observations **(D)** in the direction parallel to the main water flow. Auto- and cross-correlation functions of species distribution patterns from model simulations **(E)** and field observations **(F)** in the direction perpendicular to the main water flow. In C and E, *black lines* are the autocorrelation functions for the simulated spatial patterns of P_f; *blue lines* are the cross-correlation functions between P_f and P_b. In D and F, *black lines* are the autocorrelation functions for *Callitriche platycarpa*; *blue lines* are the cross-correlation functions between *Callitriche* and *Groenlandia*. Closed dots represent significant values.

Figure 5. Relationship between flow velocity within and around *C. platycarpa* patches, and size increase of transplanted individuals of **(A)** *B. erecta* and **(B)** *G. densa* during the experimental period (t = 49 days).

Figure 6. Relationships between flow velocity within and around *C. platycarpa* patches, and traits of vegetative reproduction for *Berula erecta* **(A, C)** and *Groenlandia densa* **(D, F)** at the end of the experiment (t = 49 days). Relationship between mother and daughter ramet height for *Berula erecta* (**B**) and *Groenlandia densa* (**E**).

Figures

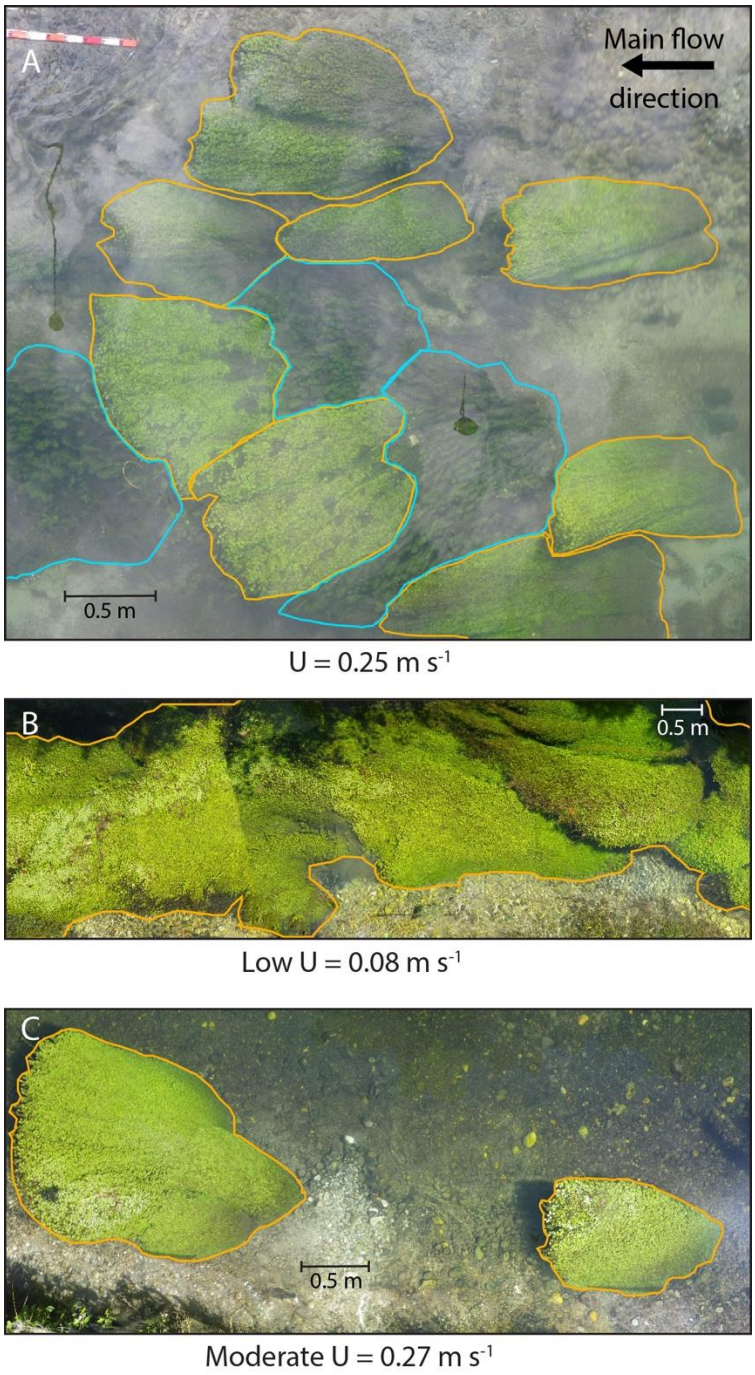

Figure 1.

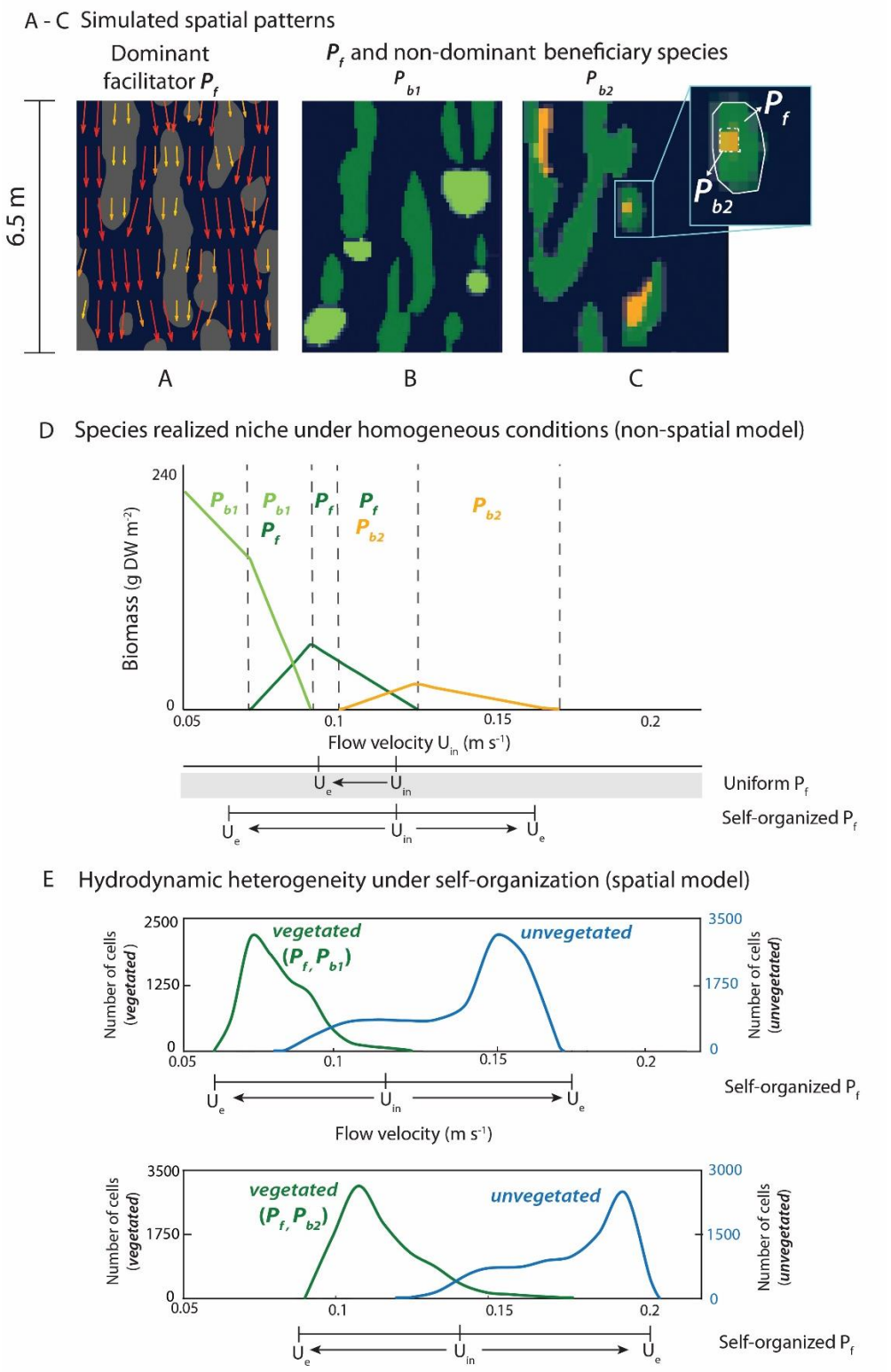
A - C Simulated spatial patterns
Dominant facilitator P_f
P_f and non-dominant beneficiary species
P_{b1}
P_{b2}
6.5 m
A
B
C
D Species realized niche under homogeneous conditions (non-spatial model)
Biomass (g DW m^{-2})
240
0
0.05
0.1
0.15
0.2
Flow velocity U_{in} (m s^{-1})
Uniform P_f
Self-organized P_f
E Hydrodynamic heterogeneity under self-organization (spatial model)
vegetated (P_f, P_{b1})
unvegetated
Number of cells (vegetated)
Number of cells (unvegetated)
2500
1250
3500
1750
Self-organized P_f
Flow velocity (m s^{-1})
vegetated (P_f, P_{b2})
3000
1500

Figure 2.

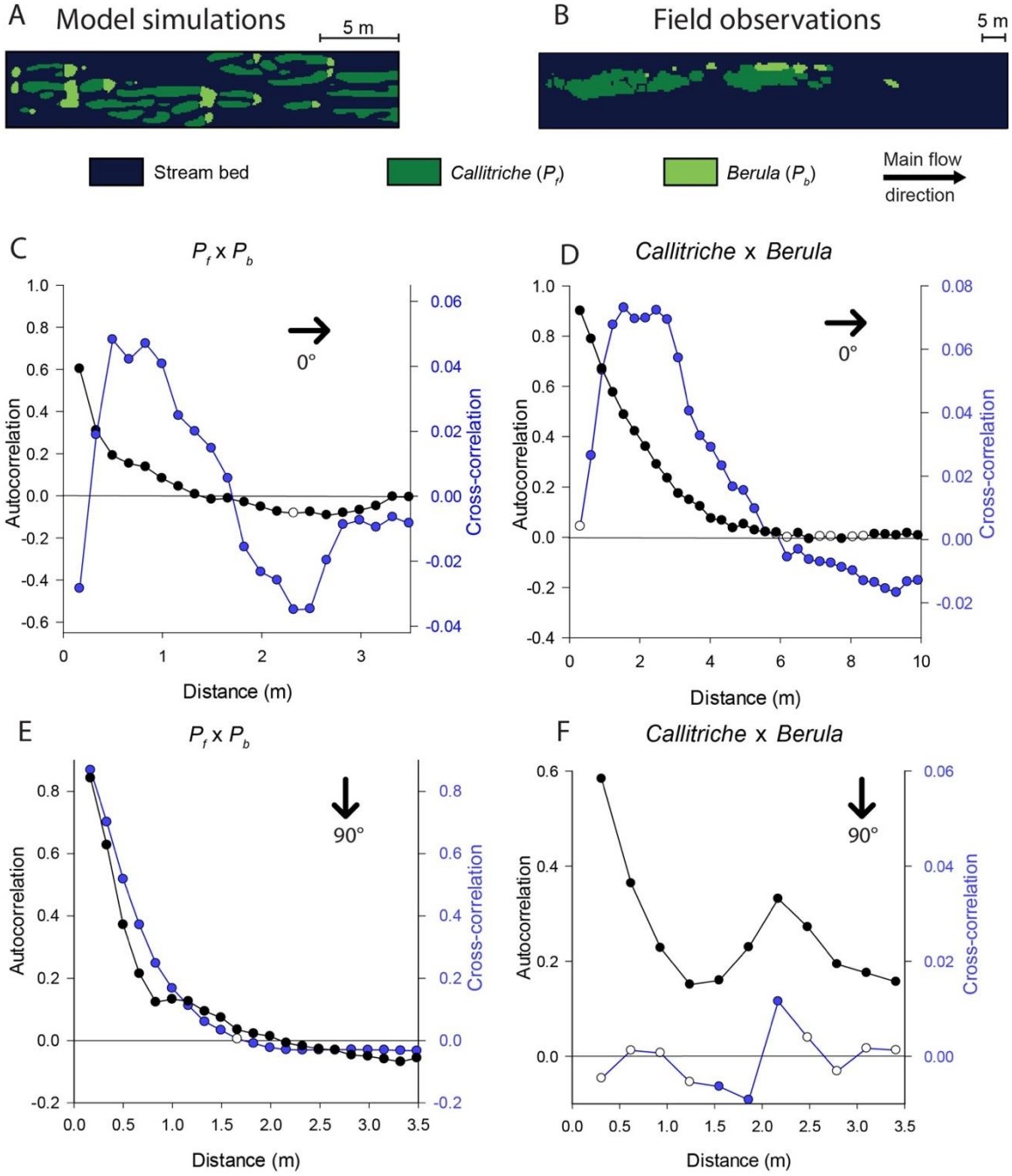
A
Model simulations
5 m
B
Field observations
5 m
Stream bed
Callitriche (P_f)
Berula (P_b)
Main flow direction
C
P_f x P_b
0°
Autocorrelation
Cross-correlation
Distance (m)
D
Callitriche x Berula
0°
Autocorrelation
Cross-correlation
Distance (m)
E
P_f x P_b
90°
Autocorrelation
Cross-correlation
Distance (m)
F
Callitriche x Berula
90°
Autocorrelation
Cross-correlation
Distance (m)

Figure 3.

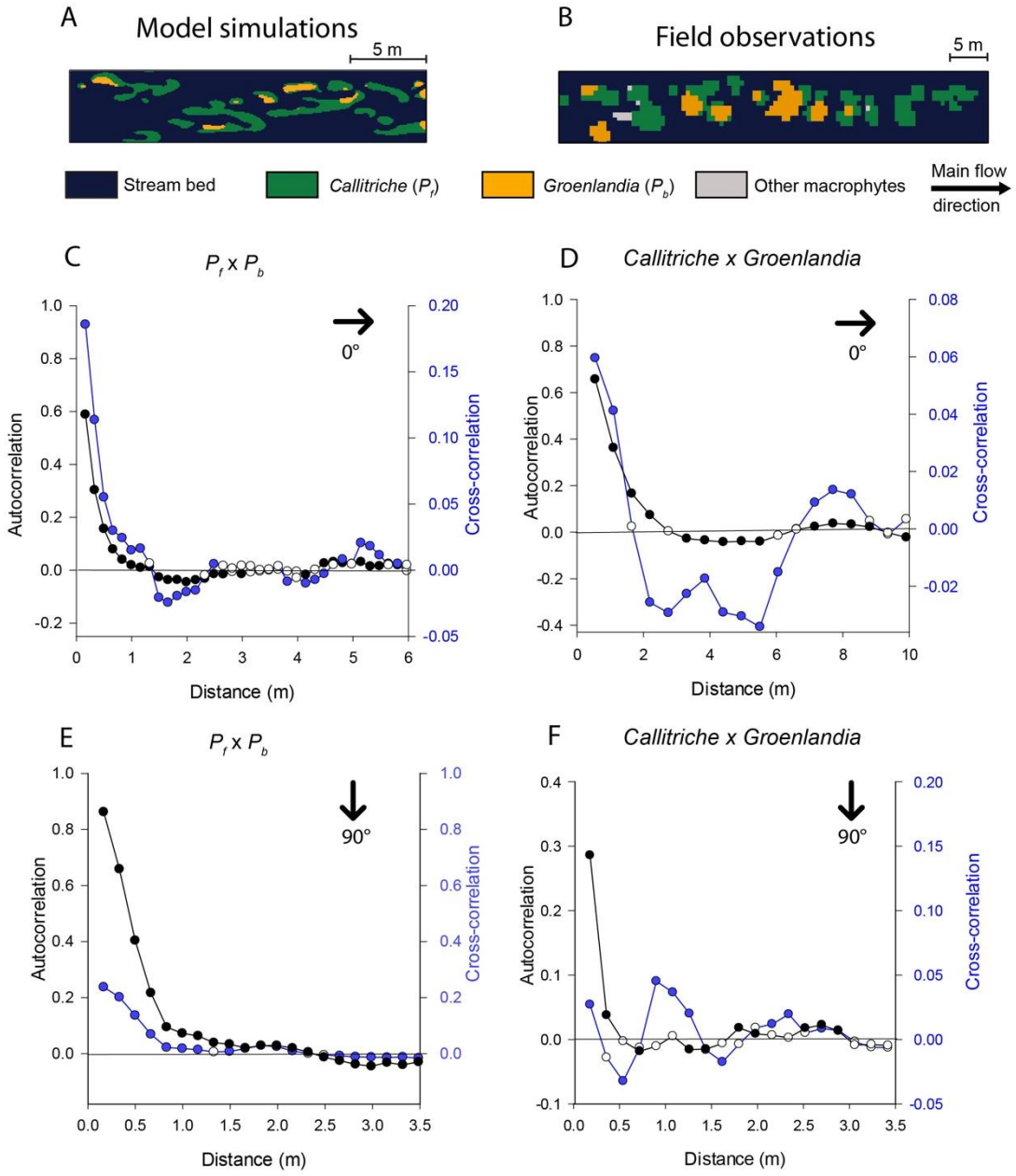
A
Model simulations
5 m
B
Field observations
5 m
Stream bed
Callitriche (P_f)
Groenlandia (P_b)
Other macrophytes
Main flow direction
C
P_f x P_b
0°
Autocorrelation
Cross-correlation
Distance (m)
D
Callitriche x Groenlandia
0°
Autocorrelation
Cross-correlation
Distance (m)
E
P_f x P_b
90°
Autocorrelation
Cross-correlation
Distance (m)
F
Callitriche x Groenlandia
90°
Autocorrelation
Cross-correlation
Distance (m)

Figure 4.

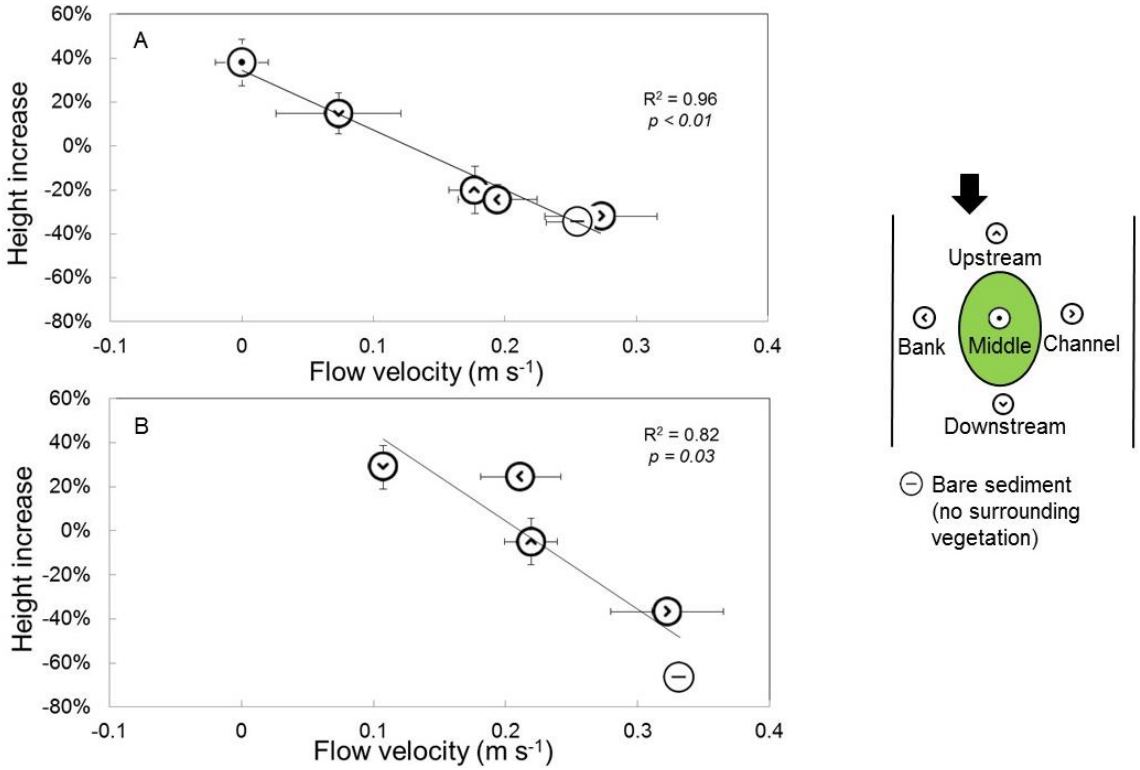
A
B
Height increase
Flow velocity (m s-1)
R2 = 0.96
p < 0.01
R2 = 0.82
p = 0.03
Upstream
Bank
Middle
Channel
Downstream
Bare sediment
(no surrounding
vegetation)

Figure 5.

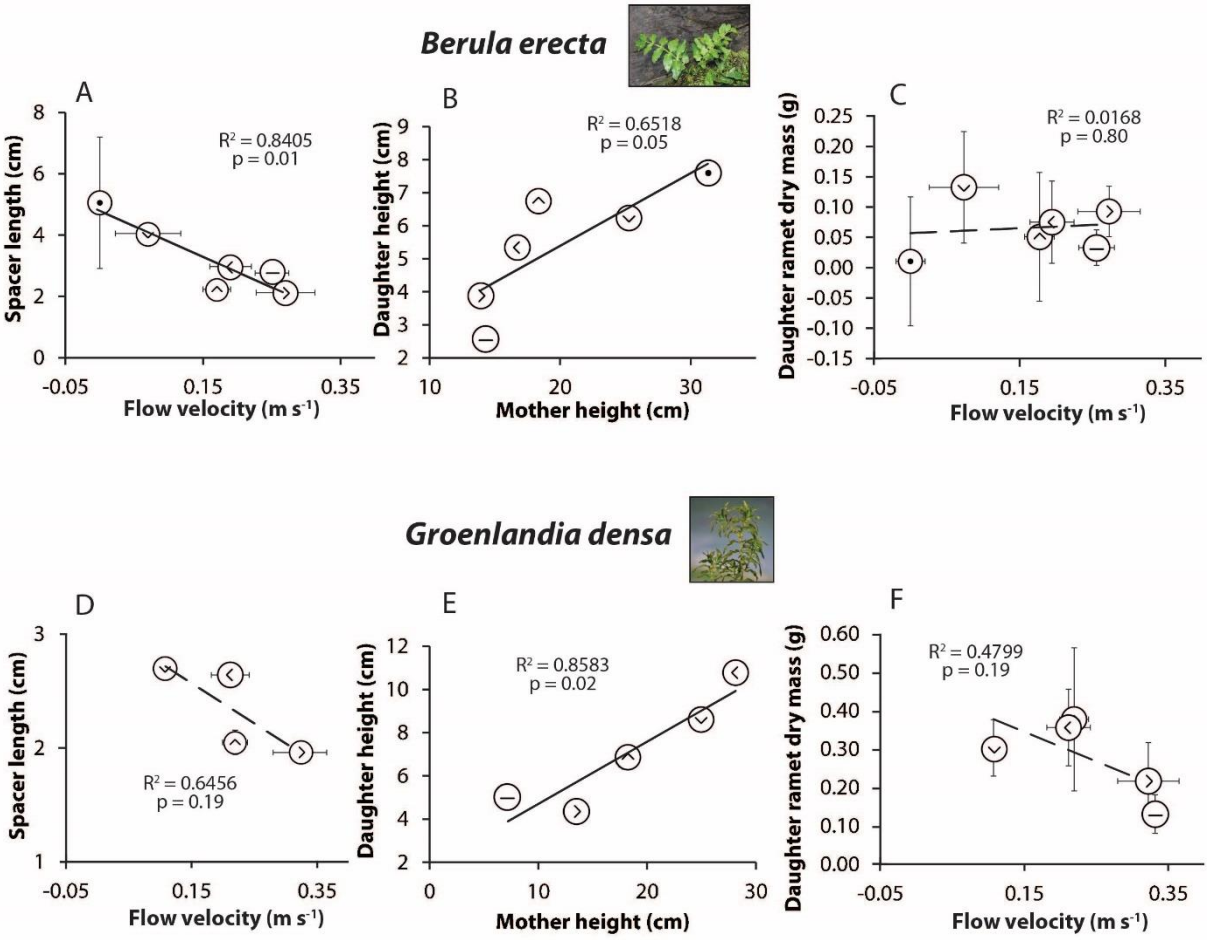
Berula erecta
A
Spacer length (cm)
Flow velocity (m s-1)
R² = 0.8405
p = 0.01
B
Daughter height (cm)
Mother height (cm)
R² = 0.6518
p = 0.05
C
Daughter ramet dry mass (g)
Flow velocity (m s-1)
R² = 0.0168
p = 0.80
Groenlandia densa
D
Spacer length (cm)
Flow velocity (m s-1)
R² = 0.6456
p = 0.19
E
Daughter height (cm)
Mother height (cm)
R² = 0.8583
p = 0.02
F
Daughter ramet dry mass (g)
Flow velocity (m s-1)
R² = 0.4799
p = 0.19

Figure 6.

Supporting Information

Appendix S1

Quantifying dispersal capabilities in relation to flow stress through clonal growth traits

For the two beneficiary species *Berula erecta* and *Groenlandia densa*, we measured clonal growth traits by sampling individuals growing aggregated into patches over a range of incoming flow velocities in the field, in order to *i)* test whether their dispersal through vegetative propagation could be described by the diffusion approximation, and *ii)* as input to parameterize the diffusion constants D_{Pi} in the model.

Different patches were selected for sampling, based on differences in local incoming flow velocity (n = 4 for *B. erecta*, n = 5 for *G. densa*). For five different positions inside the patch (upstream, downstream, and halfway in the length of the patch on the left side, middle and right side), we collected 5 clones (hereby defined as a set of physically interconnected individuals, or ramets). Plants were kept for no more than 48 hours before measurements were made. For each clone, spacer length (cm) was measured as the distance between consecutive individuals. Cumulative frequency distributions of spacer lengths were calculated for clones located in the upstream part of the patch, in order to test whether they could be described by Brownian motion (Figure S1A, B). The average spacer length was calculated as the mean over the five replicated clones, in order to analyze the relationship between step length and incoming flow velocity (Figure S1C, D).

Spreading strategies of *B. erecta* and *G. densa* revealed that *B. erecta* presents a more diffusive behavior, with larger distance between individuals at low flow velocity and individuals growing closely together at high flow velocity (Figure S1A). On the other hand, *G. densa* has a less diffusive behavior, with small spacers irrespective of flow velocity (Figure S1B). Average spacer lengths in the clones are negatively correlated with incoming flow velocities for *B. erecta* ($r^2 = 0.65$, $p < 0.05$). No significant correlation was found between average spacer lengths and incoming flow velocity in *G. densa* ($r^2 = 0.0014$, $p = 0.83$).

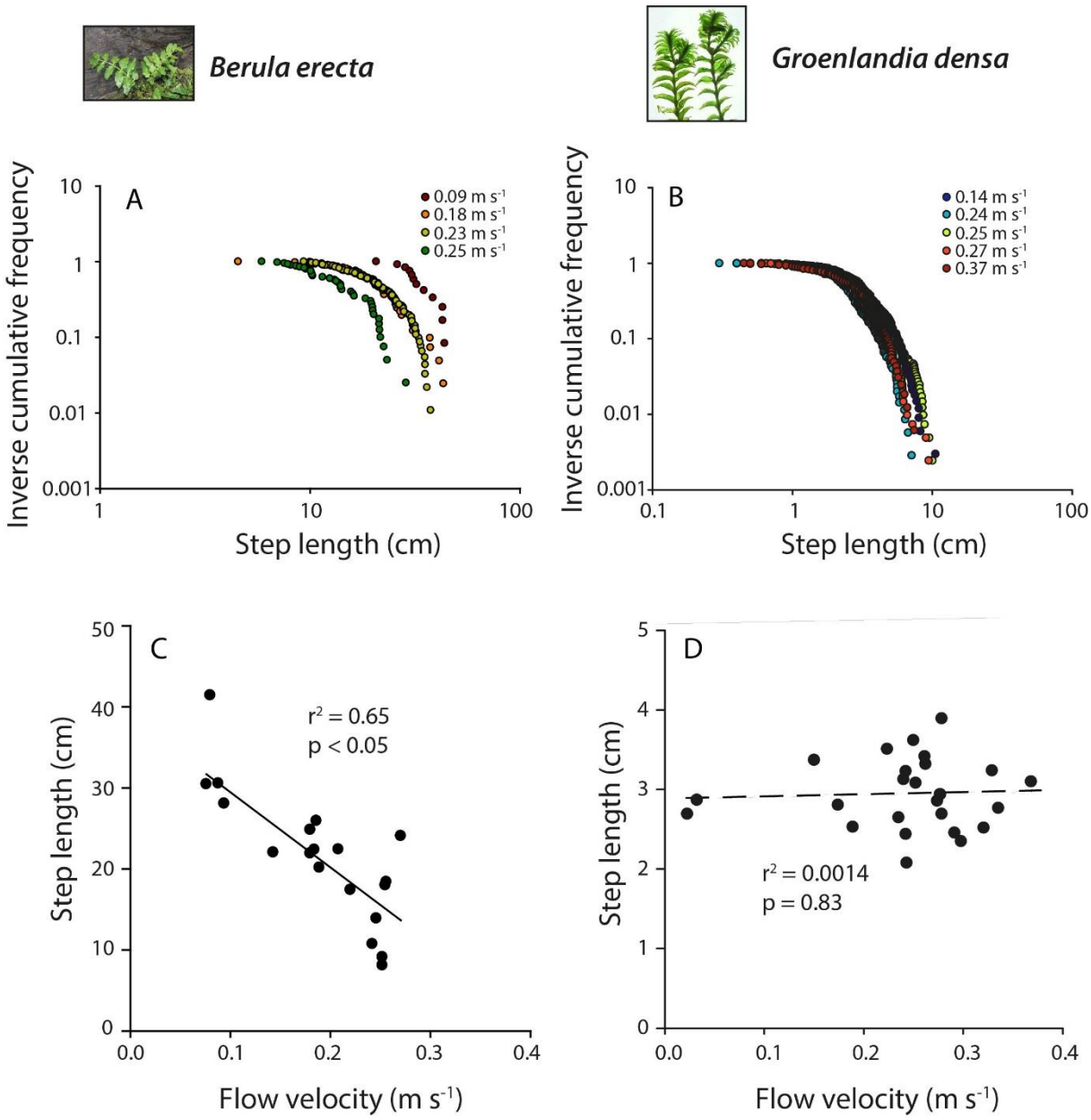

Figure S1. Cumulative distributions of step length (distance between individual plants in a clone) in patches sampled at different incoming flow velocities, and correlation between step length and incoming flow velocity for (a) *Berula erecta*, and (b) *Groenlandia densa*.

Appendix S2

Shallow water equations

Water flow is modelled using depth-averaged shallow water equations in non-conservative form (Vreugdenhil, 1989). To determine water depth and speed in both *x* and *y* directions we have:

$$\frac{\partial u}{\partial t} = -g\frac{\partial H}{\partial x} - u\frac{\partial u}{\partial x} - v\frac{\partial u}{\partial y} - \frac{g}{C_d^2}u\frac{|u|}{h} \quad \textbf{(6)}$$

$$\frac{\partial v}{\partial t} = -g\frac{\partial H}{\partial y} - u\frac{\partial v}{\partial x} - v\frac{\partial v}{\partial y} - \frac{g}{C_d^2}v\frac{|u|}{h} \quad \textbf{(7)}$$

$$\frac{\partial h}{\partial t} = -\frac{\partial}{\partial x}(uh) - \frac{\partial}{\partial y}(vh) \quad \textbf{(8)}$$

where u [m s^{-1}] is water velocity in the streamwise (x) direction, v [m s^{-1}] is the water velocity in the spanwise (y) direction, g [m s^{-2}] is the acceleration due to gravity, H [m] is the elevation of the water surface (expressed as the sum of water depth and the underlying bottom topography), h [m] is water depth and C_d [m$^{1/2}$/s] is the Chézy roughness coefficient due to bed and vegetation roughness.

The effects of bed and vegetative roughness on flow velocity are represented by determining hydrodynamic roughness characteristics for each cover type separately using the Chézy coefficient, following the approach of Straatsma & Baptist (2008) and Verschoren et al. (2016). The Chézy coefficient within the unvegetated cells of the simulated grid, which we refer to as C_b, is calculated using Manning's roughness coefficient through Equation 3 in the main text. The Chézy coefficient for each grid cell occupied by submerged vegetation, which we refer to as C_d, is calculated using Equation 4 in the main text.

Appendix S3

Location of the study sites for spatial pattern analyses and field transplantations

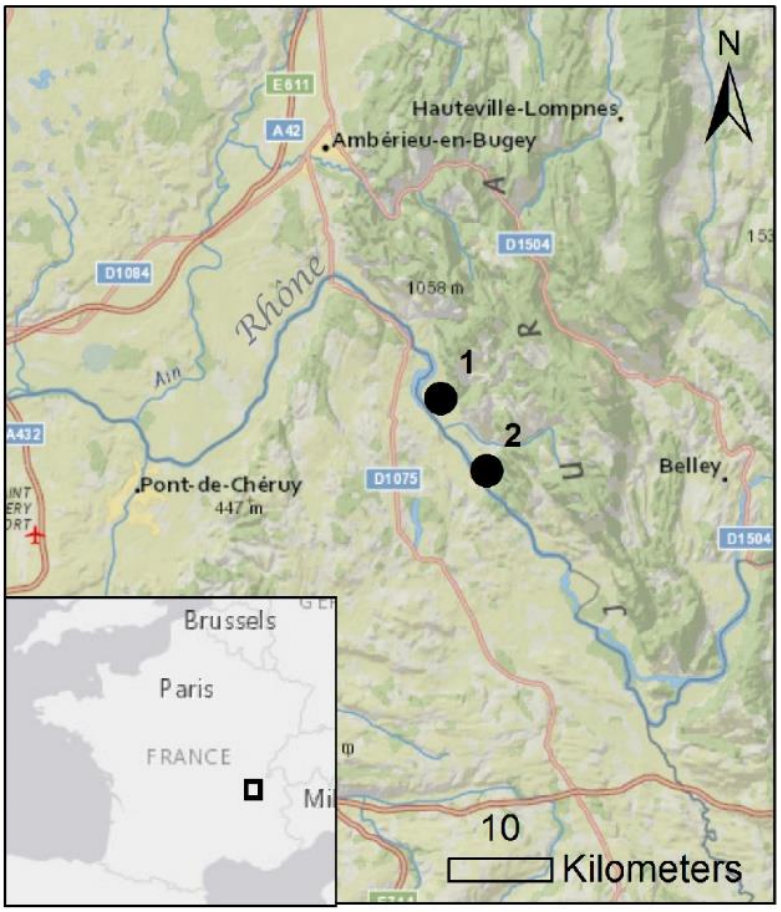

Figure S1. Location of the two study sites along the Rhône river, France (1: Serrières-de-Briord; 2: Flévieu). In both sites, aerial photographs were taken for the analysis of species coexistence patterns. Site 1 was also the location of the field transplantation experiment. *Sources: National Geographic, Esri, DeLorme, HERE, UNEP-WCMC, USGS, NASA, ESA, METI, NRCAN, GEBCO, NOAA, iPC* (main map)*; Esri, DeLorme, HERE, MapmyIndia* (inset map).

Appendix S4

Temporal flow velocity measurements in the transplantation site

Temporal flow velocity measurements collected prior to the experiment (in June 2014) and in the following summer (June – July 2015) show that summer flows in the transplantation site (Serrières-de-Briord) are stable over time. In 2014, the depth- and time-averaged velocities were measured upstream (1 m ca.) of patches of *Callitriche platycarpa*. Profiles were measured using a 3D acoustic Doppler velocimeter (ADV; FlowTracker, SonTek). Different dates refer to different patches. In 2015, the measurements are replicates of the same vertical flow velocity profile in an unvegetated location in the channel. Profiles were measured with a 3D acoustic Doppler velocimeter (ADV Vectrino, Nortek) over 2 min at 10 Hz, at five vertical locations at 5, 10, 20, 40 and 90% of the water surface elevation above the river bed. The flow velocities are shown in Figure S1.

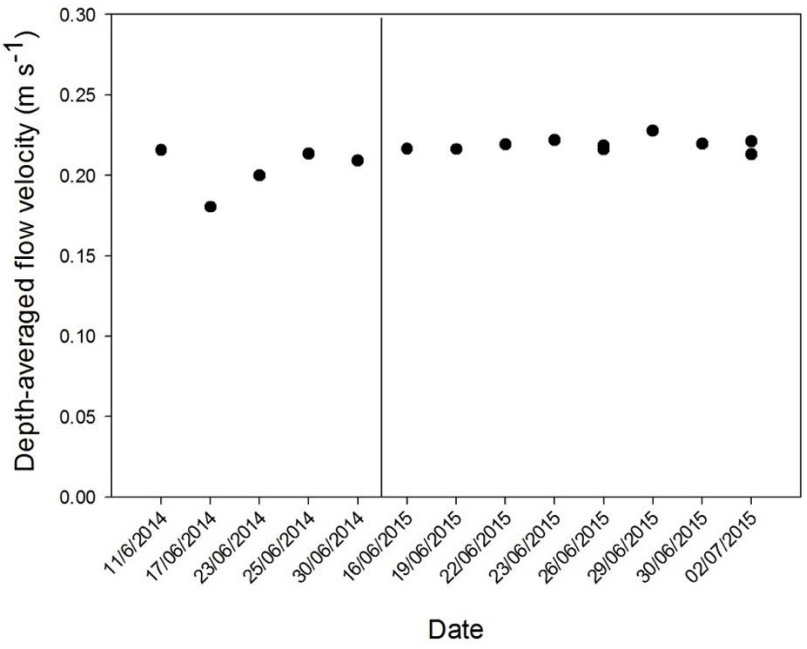

Figure S1: Depth- and time-averaged flow velocity measurements of unvegetated profiles in Serrières-de-Briord, collected during summer 2014 (before the experiment, on the left; mean ± SD: 0.204 ± 0.014 m s^{-1}) and 2015 (after the experiment, on the right; mean ± SD: 0.219 ± 0.004 m s^{-1}).

Appendix S5

Daily rainfall recorded during the experimental period

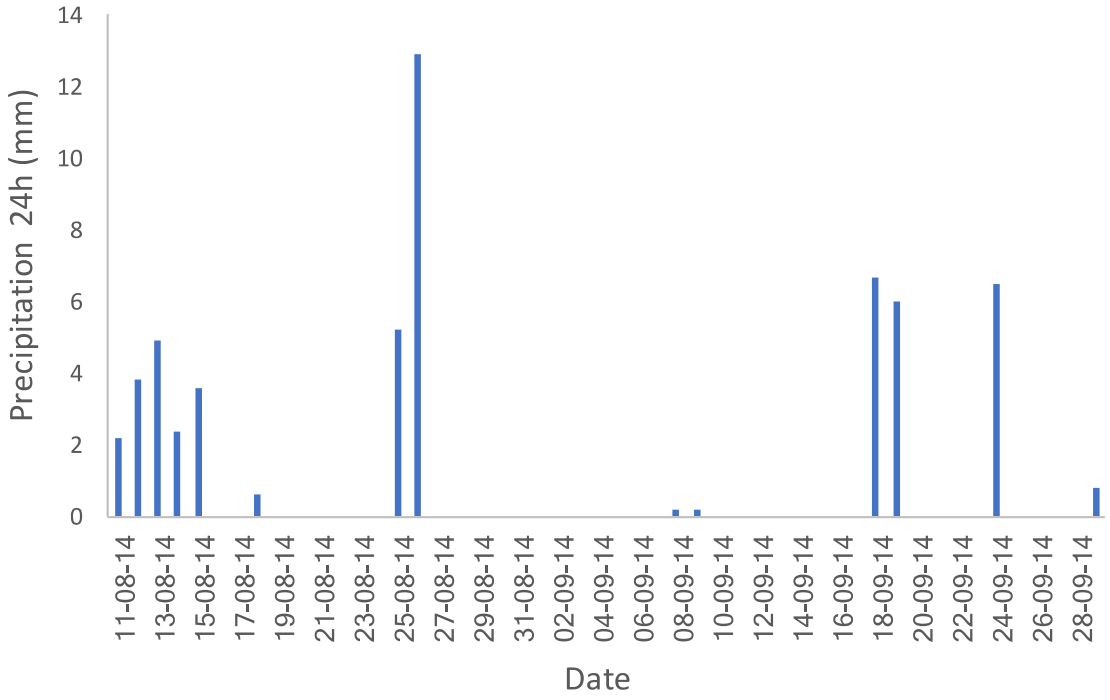

Figure S1. Daily rainfall data recorded at the weather station of Ambérieu-en-Bugey, at about 25 km from the field sites (source: http://www.meteociel.fr/climatologie/climato.php).

Appendix S6

Correlation between plant height and biomass in the study species

To test the relationship between plant height and biomass for the studied species, 15 individuals per species were collected from different patches in the channel of Serrières-de-Briord, in July 2014. Based on this strong and significant correlation, we considered shoot height instead of biomass as a good quantitative measure for growth rate in the transplantation experiment.

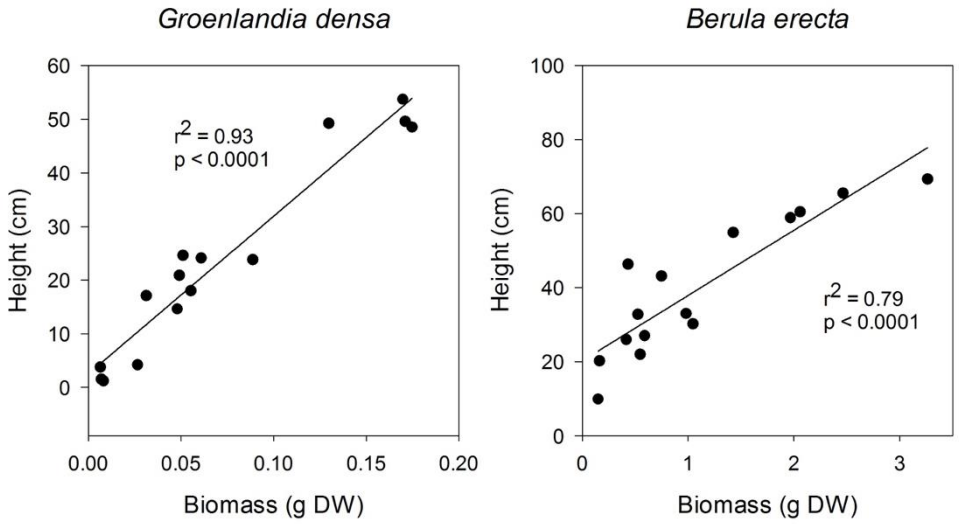

Figure S1. Biomass (g dry weight) and plant height (cm) relationship based on sampled individuals of *Groenlandia densa* and *Berula erecta* (n = 15 per species).